AN ABSTRACT OF THE THESIS OF

Surin Ruttanapaibooncharoen for the degree of Master of Science in Electrical and Computer Engineering presented on December 12, 2003.

Title: Improved Efficiency in Medium-Power Flyback Converters.

Abstract approved:

Redacted for Privacy

Annette von Jouanne

Switch-mode power supplies (SMPS's) not only convert energy, they also consume it. Typical operational efficiencies are approximately 25 to 60 % for linear power supplies, and approximately 50-90% for switching power supplies. This means that products whose end-use electronics are dc, such as televisions and DVD players, could consume 50% less power when operating if the power supply were upgraded from 40% efficiency to 80% efficiency. Savings can occur not only from using SMPS's instead of linear power supplies, but also from specifying highly efficient switching power supplies. In many cases, efficiencies are still lagging to keep costs down, since the power consumption is considered to be relatively low (40W-700W range). Over time, however, efficiency improvement strategies will pay back based on the cost of energy. Therefore three common flyback converter topologies have been studied through this thesis in the Low (15W), Medium (40W), and High (150W) Power levels. Efficiency analysis on the three power level topologies showed that the greatest opportunity for efficiency improvement existed in the 40W (medium power) topology. Efficiency improvement and measurement approaches are investigated and an optimized medium-power flyback converter is proposed and implemented resulting in an efficiency improvement from 57.8% to 83.6%.

Improved Efficiency in Medium-Power Flyback Converters

By

Surin Ruttanapaibooncharoen

A THESIS

Submitted to

Oregon State University

In partial fulfillment of the

requirements for the degree of

Master of Science

Completed December 12, 2003

Commencement June 2004

Master of Science thesis of Surin Ruttanapaibooncharoen presented on December 12, 2003.

APPROVED:

Redacted for Privacy

Major Professor, representing Electrical and Computer Engineering

Redacted for Privacy

Director of The School of Electrical Engineering and Computer Science

Redacted for Privacy

Dean of the Graduate School

I understand that my thesis will become part of the permanent collection of Oregon State University libraries. My signature below authorizes release of my thesis to any reader upon request.

Redacted for Privacy

Surin Ruttanapaibooncharoen, Author

TABLE OF CONTENTS

TABLE OF CONTENTS (CONTINUED)

LIST OF FIGURES

LIST OF FIGURES (CONTINUED)

LIST OF FIGURES (CONTINUED)

LIST OF FIGURES (CONTINUED)

LIST OF TABLES

IMPROVED EFFICIENCY IN MEDIUM-POWER FLYBACK CONVERTERS

Chapter 1

INTRODUCTION TO SWITCH-MODE POWER SUPPLIES

1.1 Fundamentals of Switch-Mode Power Supplies

Switch-mode power supplies (SMPS's) are a widely applied in computer, television, telecommunication, and battery charger system etc. Fig. 1.1 presents categories of power supplies. The three major power supply technologies that can be considered within a power supply system are:

1. Linear regulators.
2. Pulse width modulated (PWM) switching power supplies.
3. High efficiency resonant technology switching power supplies.

Each of these technologies excels in one or more system parameters and must be weighed against other considerations to determine the optimum mixture of technologies that meet the needs of the final product. The power supply industry has chosen to utilize each of the technologies within certain areas of product applications as detailed in the following.

Linear regulators are used predominantly in ground-based equipment where the generation of heat and low efficiency are not of major concern and also where low cost and short design period are desired. They are popular as board level regulators in distributed power systems where the distributed voltage is less than 40 VDC [1].

PWM switching power supplies are much more efficient and flexible in their use than linear regulators. One commonly finds them used within portable products,

computer-based systems, aircraft and automotive products, small instruments, off-line applications, and generally those applications where high efficiency and multiple output voltages are required. Their weight is much less than that of linear regulators since they require less heatsinking for the same output ratings. As shown in Fig. 1.1, the fundamental switching power supply types are Buck and Boost, from which the multiple other types are derived. The flyback derivation of the Buck converter is the focus of this thesis, and thus flyback converter is emphasized in Fig. 1.1. Section 1.2 presents additional details on the various topologies.

Resonant technology switching power supplies find their place in applications where still lighter weight and smaller size are desired, and most importantly, where a reduced amount of radiated noise (interference) is desired. The common products where these power supplies are utilized are aircraft avionics, spacecraft electronics, and lightweight portable equipment and modules. The drawbacks are that this power supply technology requires the greatest amount of engineering design time and usually costs more than the other two technologies [1].

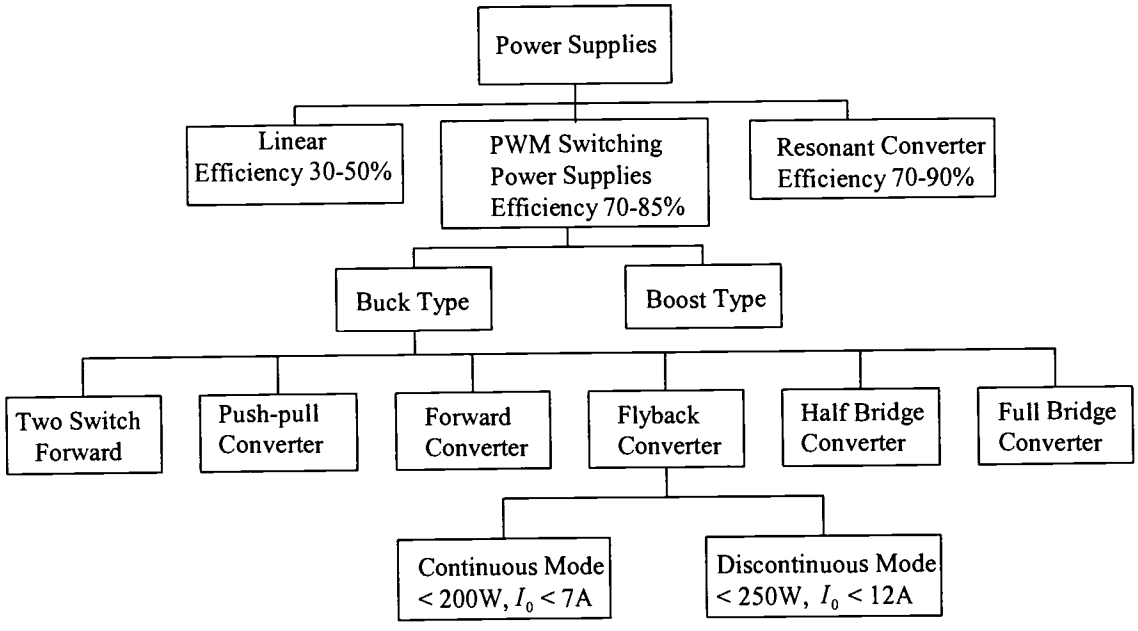

Fig. 1.1 Categories of power supplies.

Fig. 1.2 represents the block diagram of general switch-mode power supplies, including flyback converters. Advancing semiconductor technology is allowing Power MOSFET and controller circuits to be integrated into only one IC package.

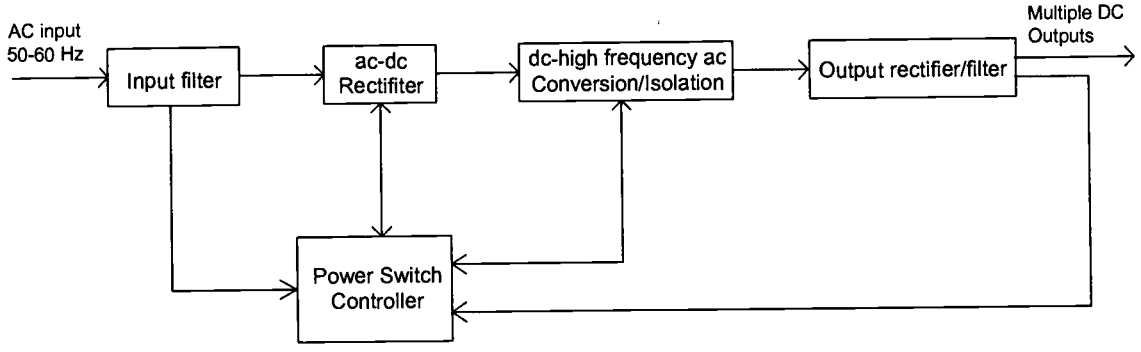

Fig. 1.2 Block diagram of a switch-mode power supply.

1.2 Topologies

There are about 14 basic topologies commonly used to implement a switching power supply. However, there are six main topologies for SMPS's [2] as shown in Fig. 1.3. Each topology has unique properties, which make it best suited for various applications. Some are best used for ac/dc off-line converters at low (<200 W) output power; some at higher output power. Some are a better choice for high ac input voltages (≥ 220 V AC); some are better for an ac input of 120 V or less. Some have advantages for higher dc output voltages (> 200 V) or in applications where there are more than four or five different output voltages. Some have lower parts count than do others for the same output power or offer a better tradeoff in parts count versus reliability. Reduced input or output ripple and noise are a frequent factor in a topology selection [3]. Table 1 gives a summary of these characteristics.

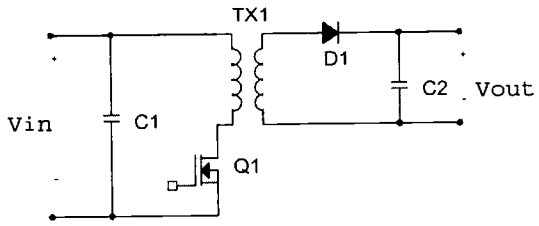

(a) Flyback

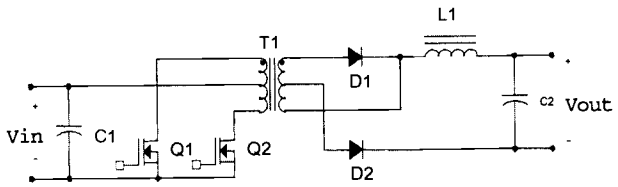

(b) Push-Pull

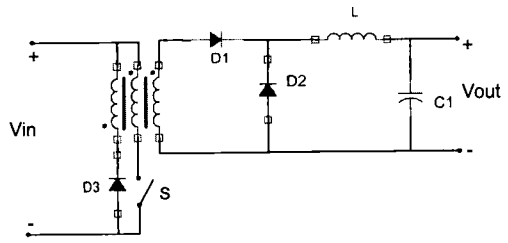

(c) Forward

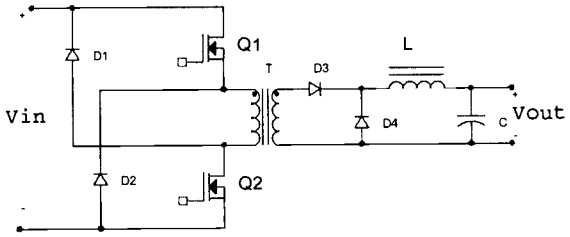

(d) Two Switch Forward

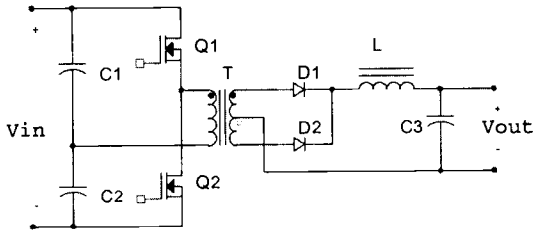

(e) Half Bridge

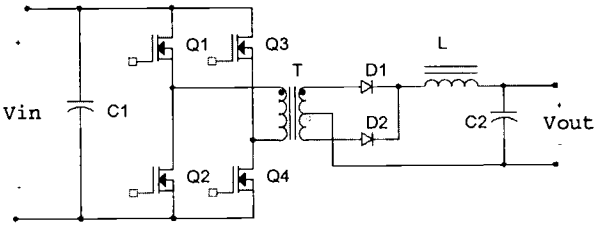

(f) Full Bridge

Fig. 1.3 Six main SMPS topologies [2].

Table 1. Comparison of the six main SMPS topologies [2].

	Advantages	Disadvantages	Typical Applications
Flyback	Drain Current reduced by turns ratio of transformer. Low parts Count. Isolation. Has no secondary output inductors.	Poor transformer utilization. Transformer stores energy. High output ripple. D1 needs fast reverse recovery.	Low output power. Supports multiple outputs. Used in television and oscilloscope circuits.
Push-Pull	Good transformer utilization. Drain current reduced as a function of the transformer turns ratio. Good at low values of V_{in}. Low output ripple	Cross conduction of switches Q_1 and Q_2 possible, high parts count. Transformer design critical. High voltage required for Q_1 and Q_2. High input current ripple.	Low input voltage.
Forward	Drain current reduced as a function of the transformer turns ratio. Low output ripple.	Poor transformer utilization. Poor transient response. Transformer design critical.Transformer reset limits duty ratio. High voltage required for Q_1. High input current ripple.	Low to moderate output power. Supports multiple outputs. Used in computer-based systems
Two Switch Forward	Drain current reduced by turns ratio. Lossless snubber recovers energy. Drain voltage ½ that of conventional forward converter. Low output ripple.	Poor transformer utilization. High part count. High side switch drive required. Transformer reset limits duty ratio. High input current ripple.	High input voltage, moderate power. Supports multiple outputs. Used in computer-based systems.
Half Bridge	Good transformer utilization. Transistors rated at V_{in}, has isolation and multiple outputs. I_{Q1} reduced as a ratio of turns ratio. High power output. Low output ripple.	Poor transient response. High parts count. C_1 and C_2 have high ripple current. Requires high side switch drive. Cross conduction of Q_1 and Q_2 possible. High input current ripple.	High input voltage, moderate-to-high power.
Full Bridge	Good transformer utilization. Transistors rated at V_{in}, has isolation and multiple outputs. I_{Q1} reduced as a ratio of turns ratio. Low output ripple	High parts count. C_1 has high ripple current. Requires high side switch drive. Cross conduction of Q_1 and Q_2 or Q_3 and Q_4 possible. High input current ripple.	High power, high input voltage

1.3 Flyback Converters

Flyback converters, see in Fig. 1.4, have a remarkably low number of components compared to other SMPS's. They also have the advantage that one control circuit can regulate several isolated output voltages. Common applications for flyback converters are TV's, DVD/VCD players, Monitors, notebook PC adapters, and battery chargers. The transistor works as a switch which is turned on and off by a pulse-width-modulated control voltage. During the on time of the transistor, the primary voltage $V_1 = V_{in}$ and I_1 increases linearly.

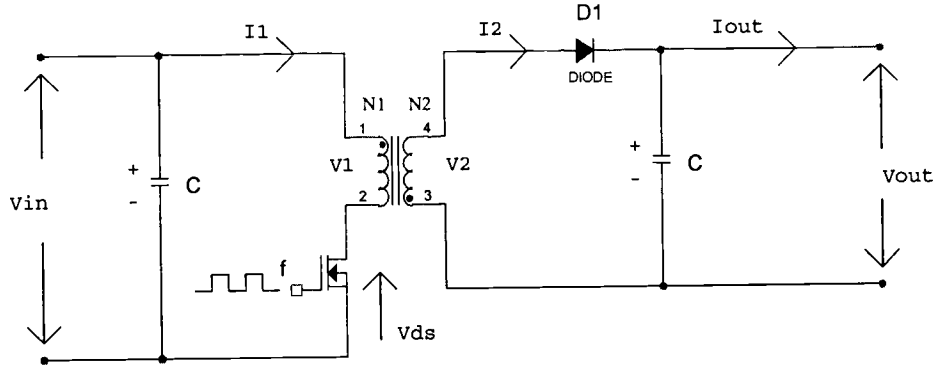

Fig. 1.4 Flyback converter.

During that phase, energy is stored in the transformer. The secondary winding does not have any current because the diode is blocking during the on-time of the transistor. When the transistor is in blocking mode then I_1 will be cut-off and the voltages at the transformer will change in accordance with Faraday's Law. The diode will then be conducting and the secondary winding will then deliver energy to the output capacitor. During the on-phase of the transistor the drain-source-voltage V_{ds} will be zero. During the off-phase the output voltage is back transformed to the primary side such that the drain-source voltage achieves the value $V_{ds} = V_{in} + V_{out} \cdot N_1/N_2$. This implies that for a flyback converter which is designed for 230V/50 Hz mains, the voltage V_{ds} usually reaches approximately 700V. In practice the voltage is even higher because an inductance voltage is added as a result of transformer leakage inductance. The transistor

in the flyback converter for the 230V mains must have a breakdown voltage of at least 800V. The transformer is not a "normal" transformer. Its function is to store energy during the on-phase of the transistor and to transfer that energy to the secondary side during the off-phase. This means that the transformer is a storage-inductor with primary and secondary windings and the transformer-core has an air-gap. Transformers for flyback converters are therefore called storage transformers. In order for the stored energy of the primary current to be transferred to the secondary winding during the off-phase of the transistor, both coils must be very well magnetically coupled.

When the transistor turns off, the magnetizing current in the primary winding stops. However, the core must now return to its previous condition of near-zero flux, and the voltage on all windings will reverse, creating the flyback action. This is the reason that the topology is named flyback and this brings the secondary windings and diodes into conduction and a decreasing (demagnetizing current) flows in the secondary.

There are two distinctly different modes of flyback converters (discontinuous and continuous) whose waveforms are shown in Fig.1.5. Both modes have an identical circuit diagram and it is only the transformer's magnetizing inductance and output load current which determines its operating mode. With a given magnetizing inductance, a circuit which has been designed for the discontinuous mode will move into the continuous mode when the output load current is increased beyond a unique boundary. The mechanism for this and its consequence is discussed below.

In the continuous mode, as seen in Fig. 1.5a, the primary current has a front-end step and the characteristic appearance of a rising ramp on a step. During the transistor off time, the secondary current has the shape of a decaying triangle sitting on a step with current still remaining in the secondary at the instant of the next turn on. There is thus still some energy left in the secondary at the instant of the next turn on.

The discontinuous mode as shown in Fig. 1.5b has no front-end step in its primary current and at turnoff the secondary current is a decaying triangle that has ramped down to zero before the net turn on. All the energy stored in the primary during the on time has been completely delivered to the secondary and thus to the load before the next turn on.

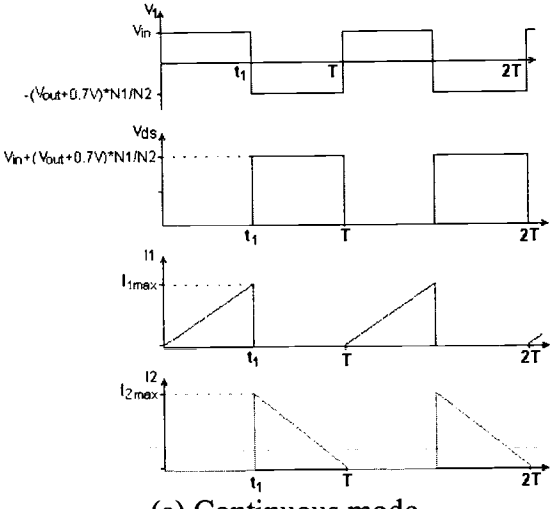

(a) Continuous mode

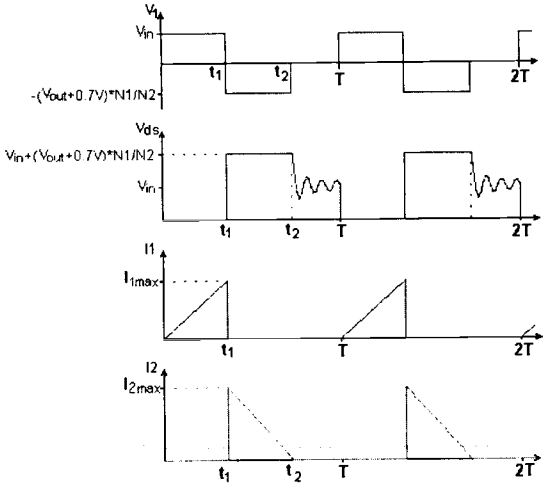

(b) Discontinuous mode

Fig. 1.5 Continuous and discontinuous mode.

How dose air gap in flyback transformer help store energy?

Increasing the air gap will swing the B/H loop more to the right, increasing the area and hence the stored energy. Most of the energy is stored in the air gap because this is the lowest permeability part of the magnetic path. The remnant flux (Br) also reduces as the core gap increase, slightly increasing the usable flux working range. The peak primary current increases as the inductance reduces. Since stored energy is proportional to $L_P \times I_P^2$, energy still increases with the larger gap even though inductance falls. The peak current and stored energy are the dependant variables set by the size of the air gap [5].

1.4 Motivation

In this thesis we will investigate three types of flyback converters, which are commonly used in household electronics. Fig. 1.6 shows the comprehensive circuit diagram of a low-power flyback converter and that of a medium-power flyback converter is shown in Fig. 1.7, a high-power flyback converter is shown in Fig. 1.8. An efficiency analysis is conducted on these three topologies and approaches are investigated in order to improve their performances.

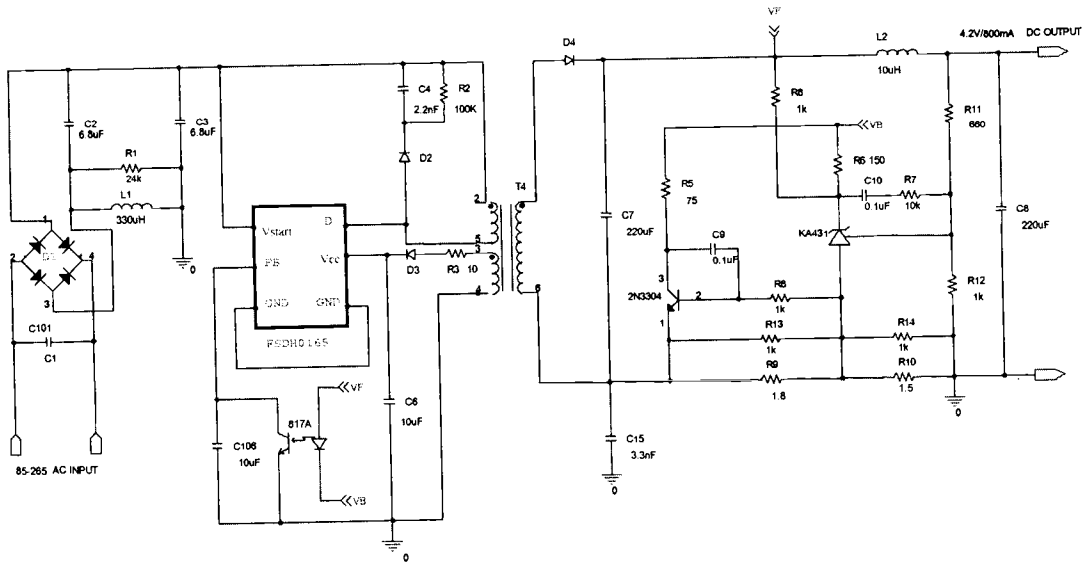

Fig. 1.6 Low-power (15W) flyback converter.

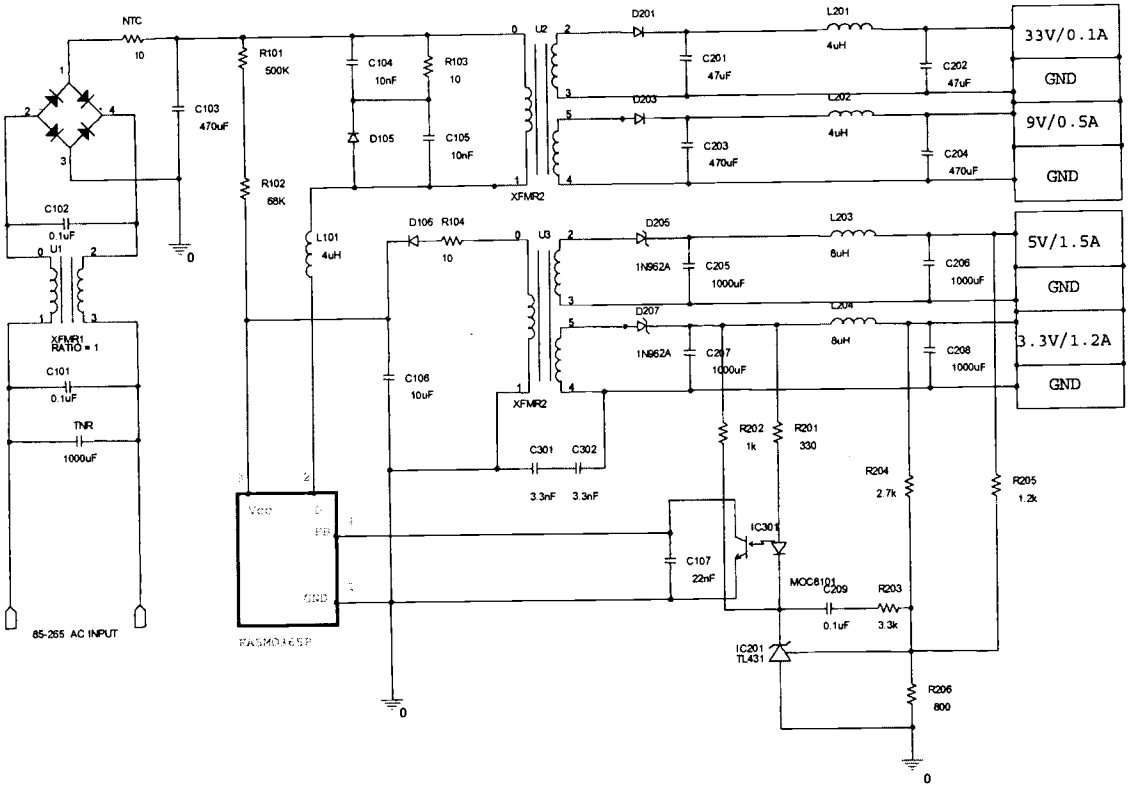

Fig. 1.7 Medium-power (40W) flyback converter.

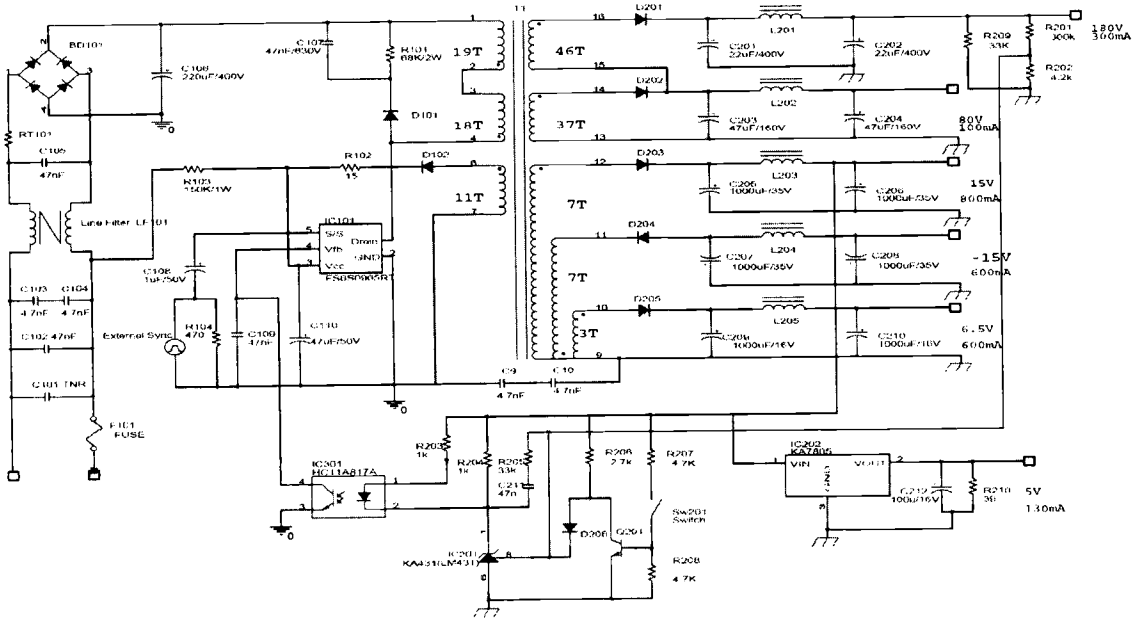

Fig. 1.8 High-power (150W) flyback converter.

Chapter 2

POWER LOSSES

2.1 Introduction

Power supplies are relatively inefficient and unfortunately much of the incoming electricity is converted to non-useful heat rather than to power the device. Nearly 2.5 billion electrical products containing power supplies are currently in use in the United States, and about 400 to 500 million new power supplies (linear and switching) are sold in the U.S. each year. The total amount of electricity that flows through these power supplies is more than 207 billion kWh/year, or about 6% of the national electric bill. More efficient designs could save an expected 15 to 20% of that energy. Savings of 32 billion kWh/year would cut the annual national energy bill by $2.5 billion, displace the power output of seven large nuclear or coal-fired power plants, and reduce carbon dioxide emissions by more than 24 million tons per year [5].

The switching power supply market is somewhat heavily concentrated in the hands of a few large manufacturers. Emerson, Tyco Electronics, and Delta Products collectively represent global sales of about $4.5 billion (33% of the total), and North American sales of about $2.9 billion (about 40% of the total). There are likewise a handful of current suppliers of the integrated circuits that greatly improve power supply efficiency [5].

How much energy is wasted by power supplies? Power supplies not only convert energy, but they also consume it. The efficiency of a power supply is determined by dividing the output power by the input power. Typical efficiencies when a product is operating are about 25 to 60% for linear power supplies and about 50 to 90% for switching power supplies. Again, this means that a product that works entirely in dc, like an answering machine, could consume 50% less power when operating if its power supply were upgraded from 40% efficiency to 80% efficiency [5]. Savings can occur not only from using switching power supplies

instead of linear, but also from specifying highly efficient switching power supplies. Efficiencies were usually higher with the original factory power supply provided with the unit than with after-market, "universal" adapters. It is simply easier to optimize a power supply for energy efficiency when it is intended to operate at a single voltage and relatively high load. To improve the efficiency of a switching system we must be able to identify and roughly quantify the various losses. Considering actual (experimental) state-of-the-art topology probe/access points, losses within a switching power supply for this work have been divided into three categories: power input, power switch and transformer, and output rectifier/filter.

2.2 Where does the energy go?

Loss - The energy lost in directly switching voltage to a capacitor at another potential is lost in parasitic resistance, and if the resistance is too low, in arcing or welding of the switch contacts, or in radiation.

Resistance - The easiest loss mechanism to show analytically is the loss in parasitic resistance, such as the capacitor equivalent series resistance (ESR) or wiring resistance. Adding this resistance to the circuit and calculating the power dissipated shows the energy loss. The energy loss is independent of the value of the resistance since energy is proportional to power and power is proportional to resistance.

Arcing - Most switches used in power supplies are solid state and arcing is not a problem, but if a capacitor is charged through a contact, arcing may be a problem.

Radiation - High rates of change of voltage or current result in radiation. Directly switching voltage to a capacitor at another potential is a source of electromagnetic interference (EMI) radiation.

2.2 Power losses associated with the power switch

Due to semiconductor technology advancements the power switches provide all of the

essential features necessary for the operation of the basic current mode controller. All logic and controller parts are integrated in only one IC package such as a high voltage power MOSFET (SenseFET) using pulse width modulation (PWM). Moreover, they provide enhanced IC functional components needed in a SMPS. This reduces a variety of components, wirings, and energy consumption. However power switches still play the major roll of introducing power dissipation loss in power supplies during switching. Therefore, the power switch is one of two of the most prominent sources of loss within the typical switching power supply. There is energy loss each time the transistor switches from one state to the other through the active region. Therefore, the power loss due to switching is linearly proportional to the switching frequency. The losses basically fall into two categories: conduction losses and switching losses. The conduction loss is where the power switch is in the ON stage after the drive and switching waveforms have stabilized. Switching losses occur when the power switch has been driven into a new state of operation. The drive and switched waveforms are in a state of transition. These periods and their typical waveforms can be viewed in the Fig. 2.1. It has been experimentally verified through this thesis work that this switching process consumes only 4% of overall losses.

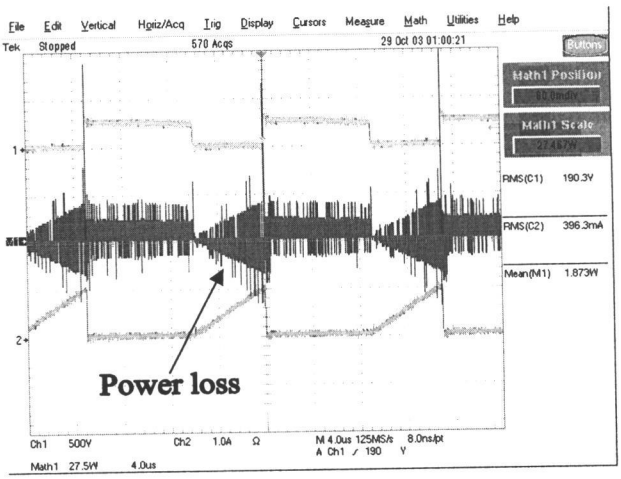

Fig. 2.1 Improved power switching operation.

This scope photo in Fig. 2.1 shows circuit operation. The switching MOSFET exhibits drain to source voltage (upper trace) and primary current (lower trace). In a real-world environment, the power supply is continuously subjected to a dynamic load. Fig. 2.1 shows that power loss at switching will also change during load/current changes. It is very important to capture the entire load-changing event and characterize the switching loss to make sure it doesn't over stress the devices.

2.4 Power losses associated with the output rectifier and filter

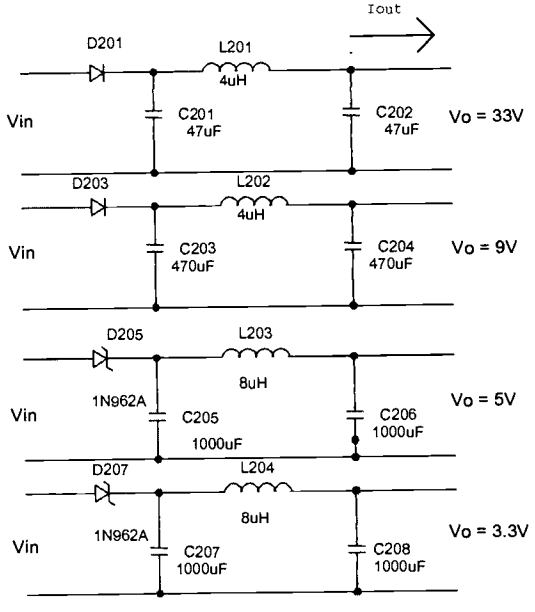

Fig. 2.2 Output rectifier and filter

The main power loss in SMPS's is found within the output rectifier and filter, which was verified through this thesis work to represent between 40 to 65 percent of the total losses [6]. The rectifier losses can be broken down into three parts: the turn-on loss, the conduction loss, and the turn-off loss. The conduction loss of a rectifier is when the current and voltage waveforms have stabilized when the rectifier is conducting. Its loss is controlled by selecting a rectifier with the lowest forward voltage drop for the operating current. P-N diodes have a more flat V-I characteristic in the forward direction, but have a fairly high voltage drop (0.7 to 1.1V). Schottky diodes have a

lower "knee" voltage (0.3 to 0.6v), but have a more resistive voltage-current characteristic. That means that the forward voltage increases more significantly with higher currents as compared to the P-N diode. During turn-on, the transition is controlled by the forward recovery characteristic of the selected rectifier. The forward recovery time (t_{rr}) is the time it takes for the diode to begin conducting forward current after a forward voltage is placed across its terminals. During the forward recovery period, the inductor or transformer has no significant load impedance because the power switch is open and the rectifier still appears open-circuited. This allows any stored energy to create ringing in its waveforms until the rectifier finally begins to conduct forward current and it clamps the power signal [8].

During the turn-off transition, the reverse recovery characteristic dominates its behavior. The carriers trapped within the junction when the reverse voltage is applied to the diode's terminals cause the reverse recovery characteristic within P-N diodes. These carriers, which have limited mobility, need to reverse direction and exit the junction from the direction they had originally come. This appears as a reverse current flowing through the diode, just after the reverse voltage is applied. The loss associated with this can be significant, because the reverse voltage can rapidly climb to very high levels before the charge has completely emptied from the junction region. The reverse current can also be reflected through any power transformer and add to the loss within the power diode during its turn-on transition [8].

The input and output capacitors, if chosen incorrectly, can make the switch mode power supply (SMSP) appear to operate less efficiently than it actually is [11]. Every capacitor has a small resistance and inductance in series with the specified capacitance of the capacitor. The equivalent series resistance (ESR) and equivalent series inductance (ESL) are parasitic elements caused by the construction of the capacitor. Both tend to isolate the internal capacitance from the signal on its terminals. Hence a capacitor will have its best characteristics at dc, but may behave more poorly at the switching frequency of the supply. The input and output capacitors are the only source of the high

frequency currents created by the power switch or the output rectifier. So, by viewing these current waveforms, we can reasonably evaluate heating within the capacitor. The major design activity surrounding filter capacitors is to assure that the internal heating of the capacitor is kept low enough to assure the product life specified for the supply. The calculation of the real power loss created by the ESR of the capacitor is given in Equation.

$$P_{D(ESR)} = (I_{SW})^2(R_{ESR}) \quad \text{input capacitor} \tag{2.1}$$

$$P_{D(ESR)} = (I_D)^2(R_{ESR}) \quad \text{output capacitor} \tag{2.2}$$

I_{SW} = Switching current.

I_D = Output rectifier current.

The inductor and transformer are the other components that will dissipate power, thereby affecting power efficiency and causing thermal runaway. Charging or discharging a capacitor may cause energy loss even if no dissipative elements are apparent.

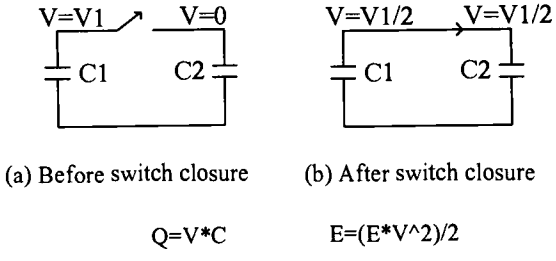

Fig. 2.3 Capacitive energy.

Fig. 2.3 (a) shows a capacitor C1 charged to voltage V1 and no voltage on capacitor C2 before switch closure. C1 is equal to C2 and the energy in the system is:

$$\text{Energy stored} = \frac{C_1 \times V_1^2}{2}$$

After switch closure (b), the charge and voltage is divided equally between the two capacitors (conservation of charge) and the total energy in the system is:

$$\text{Energy stored} = \frac{C_1 \times (\frac{V_1}{2})^2}{2} + \frac{C_2 \times (\frac{V_2}{2})^2}{2} = \frac{C_1 \times V_1^2}{4}$$

$$\therefore \text{ Energy loss} = \frac{C_1 \times V_1^2}{4}$$

Chapter 3
EFFICIENCY MEASUREMENTS

3.1 Introduction

In the past, much research has been directed at improving the efficiency of the basic PWM switching power supply. The improvements largely took the form of improved semiconductor devices and ferrite materials. Their contributions allowed the switching frequencies to rise and their efficiency to improve about another 5 to 10 percent over the bipolar transistor-based designs (SenseFET) [5]. The most recent techniques include the use of resonant and charge redirection techniques. These modifications along with the use of synchronous rectifiers, allowed switching power supplies to routinely exceed 85 percent efficiency [8]. The ultimate goal of the recent circuit techniques is to reduce or eliminate the voltage-current product, primarily during the switching transitions. This "tuning" of the waveforms inside the basic PWM converter can add about +5 to +10 percent efficiency to the supply. The tuning process, though, can add a significant amount of time to the development process. Care must be taken so that the rapid switching of charge within the power sections of the supply does not create more sources of EMI. The printed circuit board design also becomes a significant factor in the overall design of the supply. For the purpose of improving efficiency, any energy that has been redirected away from the power stages must be reinserted back into the power section in a place where the energy can be recovered. Otherwise there will be no improvement in efficiency. So, a good understanding of both the supply's operation and the tuning circuit being placed into it, is necessary to take advantage of the benefits.

3.2 Efficiency measurements

In order to investigate the significant losses and improve the efficiency of the power supply, detailed measurements will be conducted on three topologies: low-power flyback converter, medium-power flyback converter, and high-power flyback converter. In addition, we will examine each individual topology by dividing it into three stages,

i.e., the input stage (stage 1) including input filter, the middle stage (stage 2, power switch and PWM controller), and the output rectifier and filter stage (stage 3) as clearly shown in Fig. 3.1 for the medium-power topology. This will allow us to focus on the most beneficial direction for efficiency enhancement. Therefore, All measurement processes will be as follows.

A.) Low-power flyback measurement process (refer to Fig. 1.6)

We start with the first measurement stage obtaining the input and output power by using TDS7000 series oscilloscope. The two oscilloscope channels used to capture the voltage and current waveforms. For the input, we measure voltage across the input terminal and use TCP202 current probe to measure the input current at the input terminal. After that the measured input voltage and current will be employed by TDS7000 oscilloscope to obtain the mean input power. The same processes will be conducted to obtain voltages and currents for stage 2 and 3, respectively. For stage 2, input voltage was measured across C_3 and input current was measured right after the input rectifier. Similarly, for stage 3, the input voltage and current were measured across C_7 and through output rectifier D_4, respectively. From the measured voltages and currents, we will obtain mean power for each terminal to calculate for efficiency. In addition, for stage 3, the output voltage was measured across C_8 and output current was measured through load terminal. After obtaining all input and output powers, we are able to calculate for efficiencies on each stage including the overall efficiency shown in section 3.2.1.

B.) Medium-power flyback measurement process (refer to Fig. 1.7)

For stage 1, we measure the voltage across the input terminal and use TCP202 current probe to measure the input current at the input terminal. After that the measured input voltage and current will be calculated by TDS7000 oscilloscope to obtain the mean input power. The same processes will be conducted to obtain voltages and currents for stage 2 and 3, respectively. For stage 2, the input voltage was measured across C_{103} and the input current was

measured through the negative temperature coefficient (NTC) thermistor. Similarly, for stage 3, input voltages of four terminals were measured across C_{201}, C_{203}, C_{205}, and C_{207}, respectively and four input currents were measured through output rectifier D_{201}, D_{203}, D_{205}, and D_{207}, respectively. From the measured voltages and currents, we will obtain mean powers for each terminal in order for efficiency to be calculated. In addition, voltages across C_{202}, C_{204}, C_{206}, and C_{208} were respectively and four output currents were measured through each load terminal. After obtaining all input and output powers, we are able to calculate for efficiencies on each stage including the overall efficiency shown in section 3.2.2.

C.) High-power flyback measurement process (refer to Fig. 1.8)

For stage 1, we measure voltage across the input terminal and use TCP202 current probe to measure the input current at the input terminal. The same processes will be done to obtain voltages and currents for stage 2 and 3, respectively. For stage 2, the input voltage was measured across C_{106} and the input current was measured right after the input rectifier. Similarly, for stage 3, input voltages were measured across C_{201}, C_{203}, C_{205}, C_{207}, and C_{209}, respectively, and five input currents were measured through the output rectifier D_{201}, D_{202}, D_{203}, D_{204}, and D_{205}, respectively. From the measured voltages and currents, we will obtain mean powers for each terminal in order for efficiency to be calculated. In addition, for stage 3, five output voltages were measured across C_{202}, C_{204}, C_{206}, C_{208}, and C_{210}, respectively, and five output currents were measured through each load terminal. After obtaining all input and output powers, we calculate for efficiencies on each stage including overall efficiency shown in section 3.2.3.

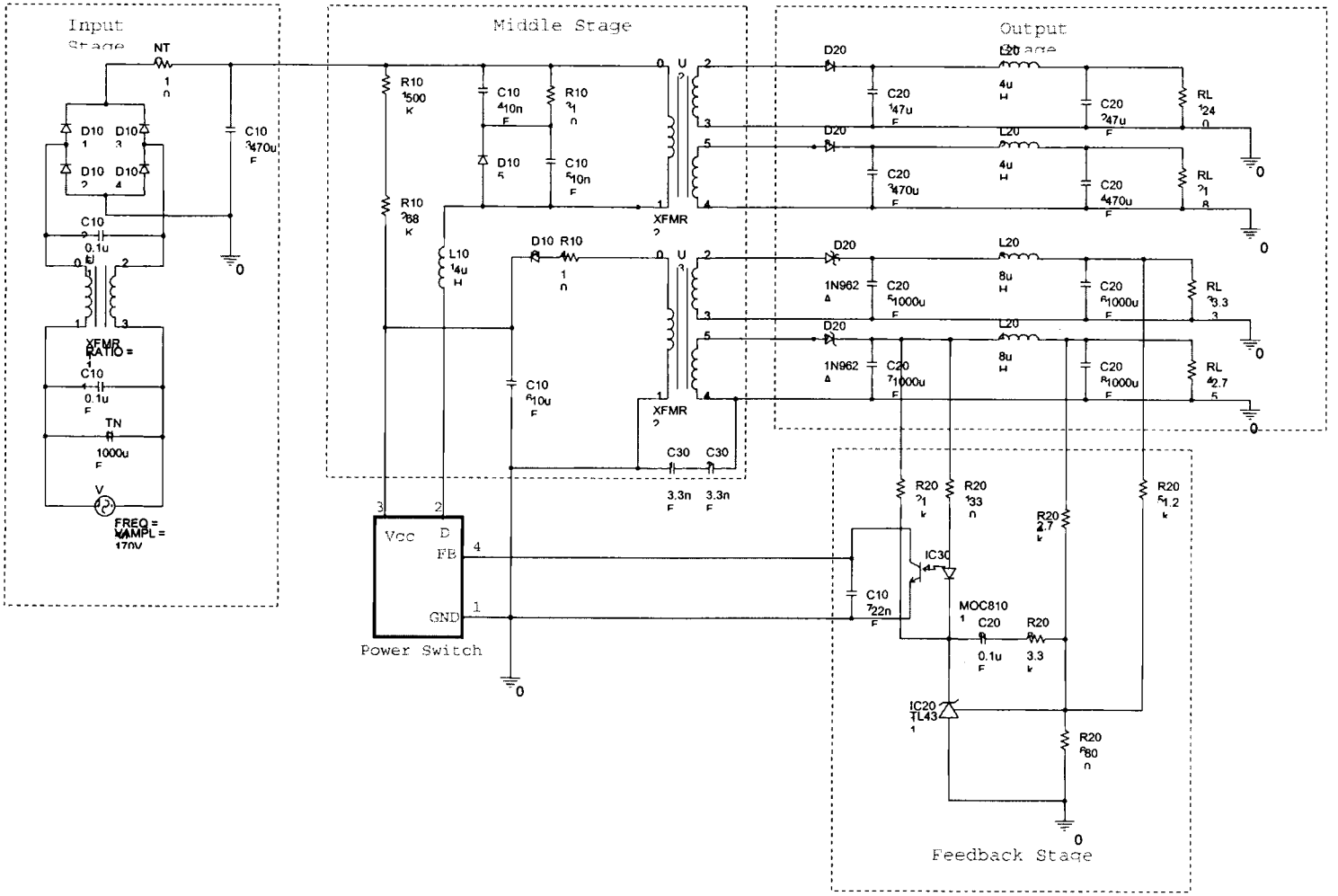

Fig. 3.1 Medium-power flyback measurement divided into separate stages

3.2.1 Low-Power Flyback Measurements

The first converter investigated is the low-power flyback converter. The schematic is shown in Fig. 3.2. In order to be able to identify the losses and efficiencies and inspect the whole efficiency, the complete converter circuit will be divided into three sections depicted in Fig. 3.3. The results of low-power flyback measurement are summarized in Table 2. This makes it possible to calculate individual efficiency for each division and the overall converter.

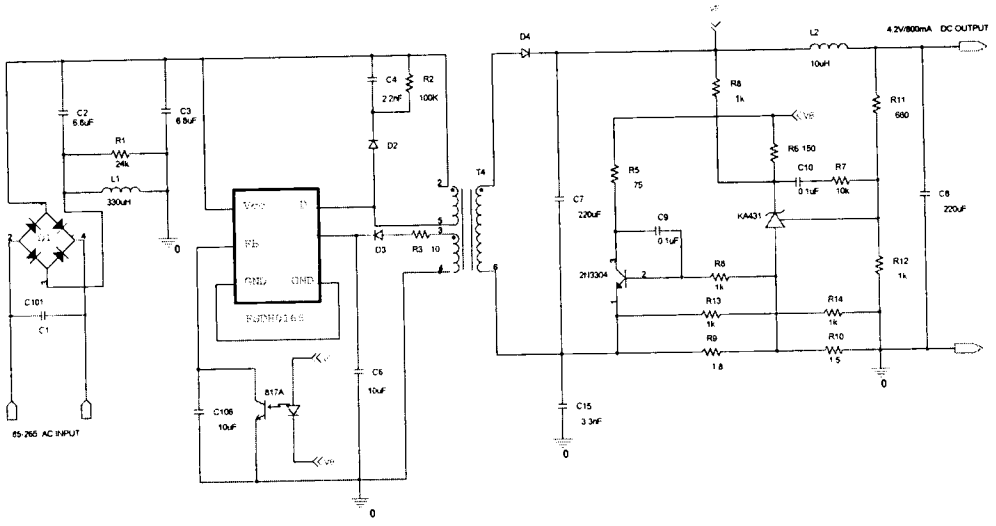

Fig. 3.2 Low-power flyback converter.

Table 2. Low-power flyback measurement results

Position	Vrms V	Irms A	P W	PF
Input	122	0.1013	6.446	0.5218
C2	152.1	0.0497	4.150	0.5486
D4	9.964	1.077	3.878	0.3614
Output 4.2V/0.8A	4.379	0.7603	3.329	1

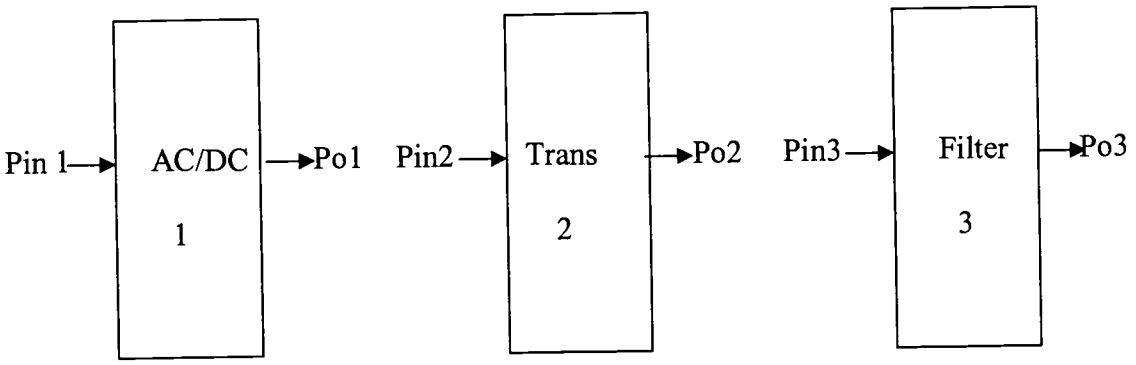

Fig. 3.3 Cascade power measurement.

From Table 2 and refer to Fig 3.3, we can calculate the efficiencies as follows.

Pin1 = 6.446 W.

Po1= 4.150 W.

Ploss1 =6.446 - 4.150 = 2.296 W.

Efficiency1 = Po1/Pin1 = 4.150 / 6.446 = 64.38%

Pin2 = 4.150 W.

Po2 = 3.878 W.

Ploss2 = 4.150 –3.878 = 0.272 W.

Efficiency2 = Po2/Pin2 = 3.878/ 4.150 =93.45%

Pin3 = 3.878 W.

Po3= 3.329 W.

Ploss3 = 3.878-3.329 = 0.541 W.

Efficiency3= Po3/Pin3 = 3.329/ 3.878 = 85.86 %

Over all
Pin = 6.446 W.

Po = 3.329 W.

Ploss = 6.446-3.329 = 3.117 W.

Efficiency = 3.329 /6.446= 51.64%

The low-power flyback converter shows an overall efficiency of 51.64%. This

percentage is considered as very low efficiency. Improved efficiency is desired for the low-power flyback converter, however the low-power hardware topology is difficult to modify due to the tight packaging.

3.2.2 Medium-Power Flyback Measurements

The schematic of the medium power flyback converter in Fig. 3.4 is divided into several stages as shown in Fig. 3.1, analogous to Fig. 3.3, in order to measure for each individual section and the results are presented in Table 3.

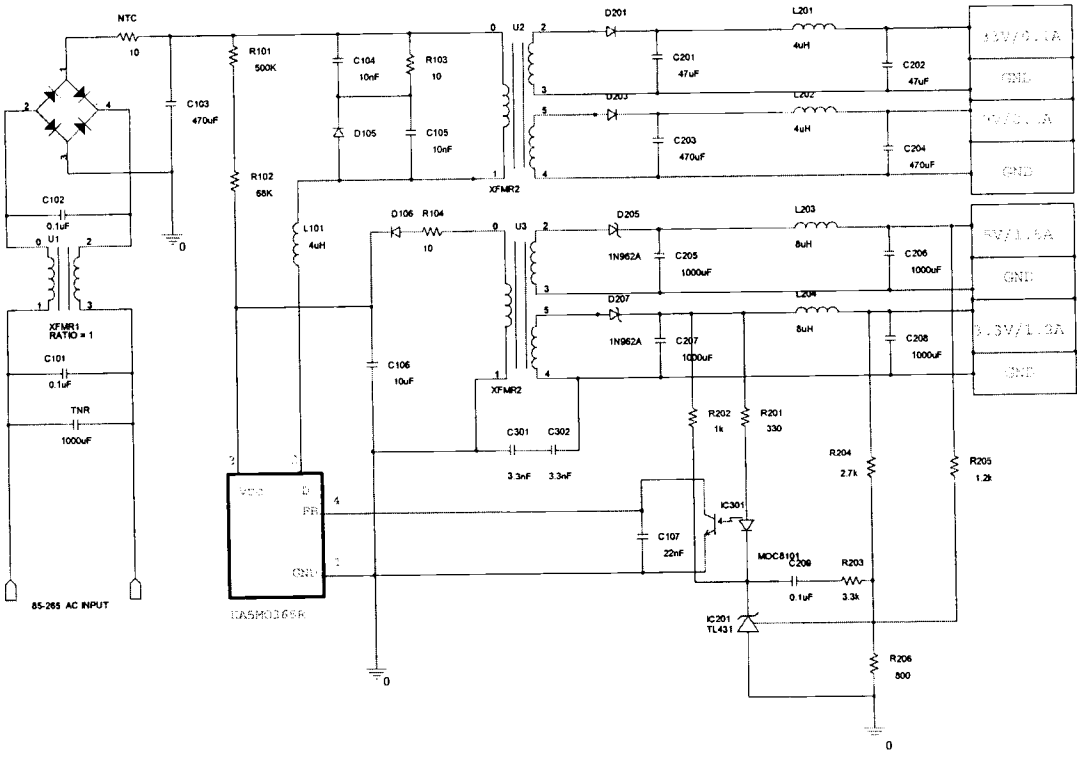

Fig. 3.4 Medium-power flyback converter.

Table 3. Meduim-power flyback measurement results.

Position	Vrms (V)	Irms (A)	P (W)	PF
Input	123.8	0.4281	33.78	0.637
NTC	153.4	0.4259	31.48	0.4818
D201	37.8	0.3762	9.401	0.661
D203	9.718	1.044	7.265	0.716
D205	5.351	2.103	7.942	0.706
D207	3.05	1.952	5.515	0.926
Output (33V/0.1A)	37.34	0.111	4.142	0.99
Output (9V/0.5A)	9.474	0.4972	4.707	0.99
Output (5V/1.5A)	5.074	1.477	7.493	0.99
Output (3.3V/1.2A)	2.933	1.082	3.172	0.99

From Table 3, we can calculate the efficiencies as follows.

Pin = 33.78W.

Po1= 31.48W.

Ploss1 =33.78- 31.48= 2.3 W.

Efficiency1 = Po1/Pin = 31.48/ 33.78= 93.19%

Pin1 = 31.48W.

Po2 = 9.401+7.265+7.942+5.515= 30.123 W.

Ploss2 = 31.48-30.123 = 1.357W.

Efficiency2 = Po2/Pin1 = 30.123 / 31.48= 95.68%

Pin2 = 30.123 w.

Po= 4.142+4.707+7.493+3.172= 19.514W.

Ploss3 = 30.123 -19.514= 10.609 W.

Efficiency3= Po/Pin2 = 19.514/ 30.123 = 64.78 %

Over all

Ploss = 33.78-19.514= 14.266 W.

Efficiency = 19.514/33.78= 57.77%

From above results, the efficiency of the medium-power flyback converter is 57.77%. This is also considered as very low efficiency. Much better efficiency is desired for the converter. The last section is rectifier and filter, with 64.78% efficiency. This indicates that the output rectifier and filter exhibits the main power loss and is thus an important issue for improved efficiency. Fortunately, the 40W (medium power) flyback converter hardware topology allows potential modifications, and thus this will be a focus of this thesis work.

3.2.3 High-Power Fly-back Converter Measurements

The schematic of the high-power flyback converter in Fig. 3.5 is divided in each stage as shown in Fig. 3.3. Measurements for each individual section and the results are shown in Table 4.

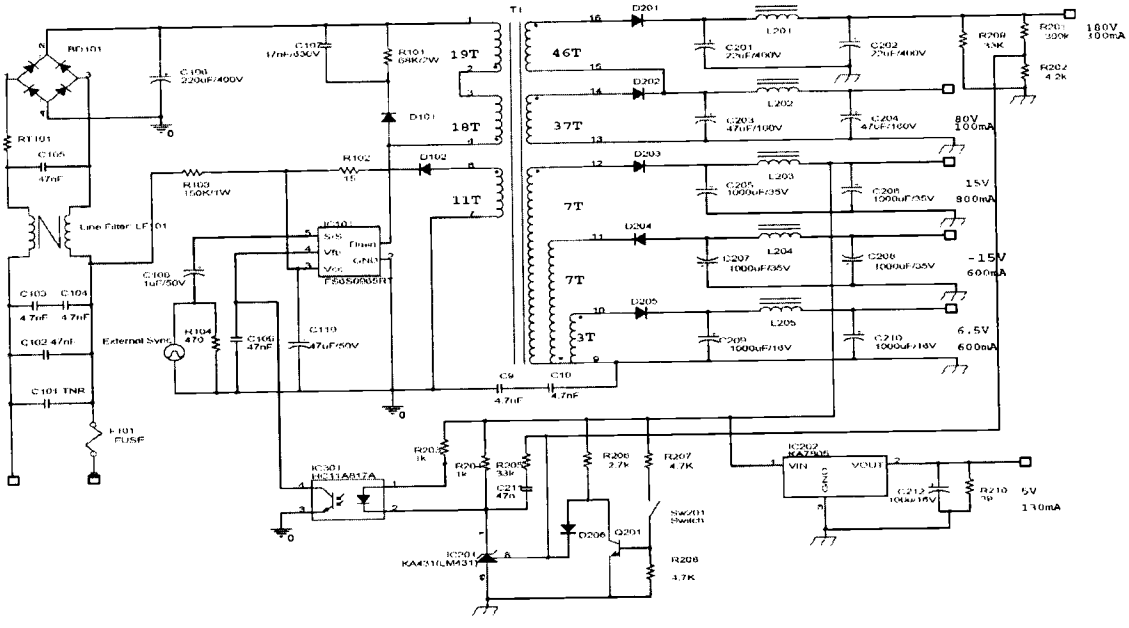

Fig. 3.5 High power flyback converter.

Table 4. High-power flyback measurement results

Position	Vrms V	Irms A	P W	PF
Input	123.1	1.53	113.1	0.907
C106	158.4	1.465	111.9	0.699
D201	185.8	0.6119	67.58	0.594
D202	81.6	0.1643	9.66	0.721
D203	15.74	1.824	20.1	0.700
D204	-13.01	1.104	-9.058	0.631
D205	7.462	0.758	4.155	0.735
Output 180V/0.3A	185.4	0.3417	63.3	0.999
Output 80V/0.1A	81.4	0.1351	10.98	0.998
Output 15V/0.8A	15.92	0.8157	12.98	0.999
Output -15V/0.6A	-12.95	-0.5534	7.156	0.998
Output 6.5V/0.6A	6.792	0.5555	3.768	0.998
Output 5V/0.13A	6.199	0.1566	0.9662	0.995

From Table 4 and referring to Fig 3.3, we can calculate the efficiencies as follows.

Pin1 = 113.1W.

Po1= 111.9W.

Ploss1 =113.1- 111.9= 1.20 W.

Efficiency1 = Po1/Pin1 = 111.9/ 113.1= 98.94%

Pin2 = 111.9 W.

Po2 = 67.58+9.66+20.1+9.058+4.155= 110.553 W.

Ploss2 = 111.9 -110.553= 1.347 w.

Efficiency2 = Po2/Pin2 = 110.553/ 111.9 = 98.796%

Pin3 = 110.553 W.

Po3= 63.3+10.98+12.98+7.156+3.768+0.9662 = 99.1502 W.

Ploss3 = 110.553-99.1502 = 11.4028 W.

Efficiency3= Po3/Pin3 = 99.1502/ 110.553 = 89.69%

Over all

Pin = 113.1 W.

Po = 99.1502 W.

Ploss = 113.1-99.1502 = 13.9498 W.

Efficiency = 99.1502 /113.1= 87.67%

From the above results, the high-power flyback converter efficiency is 87.67%. This efficiency is considered fairly high for switching power supplies. The main power loss still results from the output rectifier and filter stage. We have learned that the core-improved efficiency has to be effectively performed by developing the output stage. Therefore, we will narrow down our approach by focusing on the output filters on the next chapter.

Chapter 4

OUTPUT FILTERS

4.1 Introduction

In general the output section of any switching power supply is comprised of a single or multiple dc voltages, which are derived by direct rectification and filtering of the transformer secondary voltages and in some cases further filtering by series-pass regulators. These outputs are normally low-voltage, direct current, and capable of delivering a specified power level to drive electronic components and circuits. Most common output voltages are 5Vdc, 12Vdc, 15Vdc, or 24Vdc, and their power capability may vary from a few watts to thousands of watts. The most common type of secondary voltages that have to be rectified in a switching power supply are high-frequency square waves, which in turn require special components, such as Schottky or fast recovery rectifiers, low ESR capacitors, and energy storage inductors, in order to produce low noise outputs useful to the majority of electronic components. This chapter describes the characteristics, merits, and limitations of the components used in the output section of the switching power supply. Design equations and procedures are also developed in the practical application of these components.

4.2 What Does a Filter Do?

In circuit theory, a filter is an electrical network that alters the amplitude and/or phase characteristics of a signal with respect to frequency. Ideally, a filter will not add new frequencies to the input signal, nor will it change the component frequencies of that signal, but it will change the relative amplitudes of the various frequency components and/or their phase relationships. Filters are often used in electronic systems to emphasize signals in certain frequency ranges and reject signals in other frequency ranges. Such a filter has a gain which is dependent on the signal frequency.

As an example, consider a situation where a useful signal at frequency f1 has been contaminated with an unwanted signal at f2. If the contaminated signal is passed through a circuit (Fig. 4.1) that has very low gain at f2 compared to f1, the undesired signal can be removed, and the useful signal will remain. Note that in the case of this simple example, we are not concerned with the gain of the filter at any frequency other than f1 and f2. As long as f2 is sufficiently attenuated relative to f1, the performance of this filter will be satisfactory. In general, however, a filter's gain may be specified at several different frequencies, or over a band of frequencies. Since filters are defined by their frequency-domain effects on signals, it makes sense that the most useful analytical and graphical descriptions of filters also fall into the frequency domain. Thus, curves of gain vs. frequency and phase vs. frequency are commonly used to illustrate filter characteristics, and the most widely used mathematical tools are based in the frequency domain.

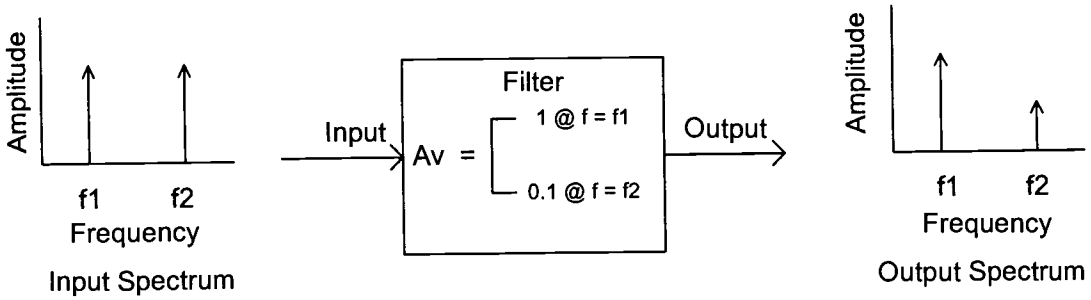

Fig. 4.1 Filter operation.

The frequency-domain behavior of a filter is described mathematically in terms of its transfer function or network function. This is the ratio of the Laplace transforms of its output and input signals. The voltage transfer function H(s) of a filter can therefore be written as:

$$H(s) = \frac{V_{OUT}(s)}{V_{IN}(s)} \tag{4.1}$$

where Vin(s) and Vout(s) are the input and output signal voltages respectively and s is the complex frequency variable. The transfer function defines the filter's response to any arbitrary input signal, but we are most often concerned with its effect on continuous sine waves. Especially important is the magnitude of the transfer function as a function of frequency, which indicates the effect of the filter on the amplitudes of sinusoidal signals at various frequencies. Knowing the transfer function magnitude (or gain) at each frequency allows us to determine how well the filter can distinguish between signals at different frequencies. The transfer function magnitude versus frequency is called the amplitude response or sometimes, especially in audio applications, the frequency response.

4.3 Output Rectification and Filtering Schemes

The output rectification and filtering scheme used in a power supply depends on the type of supply topology the designer chooses to use. The conventional flyback converter uses the output scheme shown in Fig. 4.2 Since the transformer T1 in the flyback converter also acts as an energy storage inductor, diode D1 and capacitor C1 are the only two elements necessary to produce a dc output. Some practical designs, however, may require the optional insertion of an additional LC filter, shown in Fig. 4.2 within dotted lines, to suppress high-frequency switching spikes. The physical and electrical values of both L and C will be small. An important factor in the design of any power supply output section is the minimum dc blocking voltage requirement of the rectifier diode and the freewheeling diode. For the flyback converter, the rectifier diode D1 must have a reverse voltage rating of [1.2 Vin(Ns/Np)], minimum [8].

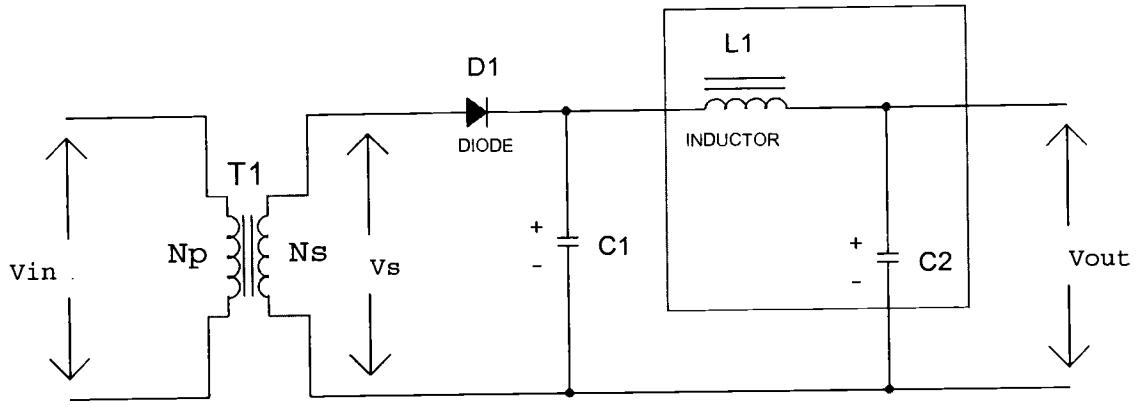

Fig. 4.2 Output section of a flyback type switching power supply.

4.4 LC Low pass Filters

The frequency response of the output filter often dictates the required feedback compensation in a switching converter. The output filter, L - C in Fig 4.3, is essentially a second-order low-pass filter. Transforming the reactive components into their S-domain parameters in Fig. 4.3 can derive the transfer function of this output filter as below.

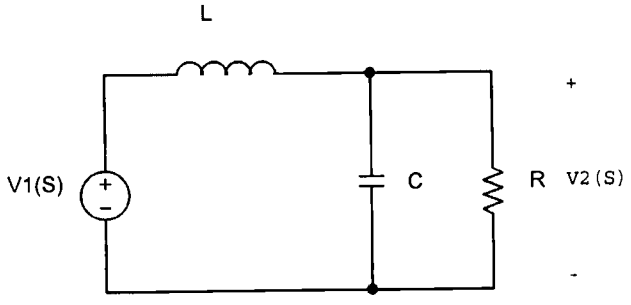

Fig. 4.3 basic LC low pass filter.

$$\frac{V_2(S)}{V_1(S)} = \frac{1}{1+\frac{S}{Qw_0}+\left(\frac{S}{w_0}\right)^2} \tag{4.2}$$

Q ≡ Quality factor of the resonant circuit. For Q ≤1/2 roots are real while for Q ≥ 1/2 roots are complex. Q is in linear units. In addition, the gain is defined as (substituting for Q and w_0):

$$G(s) = \frac{V_2(S)}{V_1(S)} = \frac{1}{1+\frac{L}{R}S+LCS^2} \tag{4.3}$$

$$G(s) = \frac{1}{1+\frac{S}{Qw_0}+\left(\frac{S}{w_0}\right)^2} \tag{4.4}$$

$$f_0 = \frac{w_0}{2\pi} = \frac{1}{2\pi\sqrt{LC}} \tag{4.5}$$

$$Q = R\sqrt{\frac{C}{L}} \tag{4.6}$$

$$w_0 = \text{Corner radian Frequency} = \frac{1}{\sqrt{LC}} \text{ or } f_0 = \frac{1}{2\pi\sqrt{LC}} \tag{4.7}$$

$$G(s) = \frac{1}{1+2\zeta\frac{S}{w_0}+\left(\frac{S}{w_0}\right)^2} \quad \text{OR} \quad \frac{1}{1+\frac{S}{Qw_0}+\left(\frac{S}{w_0}\right)^2} \tag{4.8}$$

Where ζ is the dimensionless damping ratio and w_0 is the natural frequency of the system. When $\zeta = 1$, the response is critically damped. When $\zeta < 1$, the response is underdamped. The response is increasingly oscillatory as ζ approaches zero. When $\zeta > 1$, the response is overdamped.

The following characteristics are also exhibited:

-When the coefficients of s are real and positive, then the parameters ζ, w_0, and Q are also real and positive.

-The parameters ζ, w_0, and Q are found by equating the coefficients of S

-The parameter w_0 is the angular corner frequency, and we can define $f_0 = \frac{w_0}{2\pi}$

-The parameter ζ is called the damping factor, ζ controls the shape of the exact curve in the vicinity of $f = f_0$, The roots are complex when $\zeta < 1$.

-In the alternative form, the parameter Q is called the quality factor. Q also controls the shape of the exact curve in the vicinity of $f = f_0$. The roots are complex when Q> 0.5.

In a second-order system, ζ and Q are related according to

$$Q = \frac{1}{2\zeta} \tag{4.9}$$

Q is a measure of the dissipation in the system. A more general definition of Q, for sinusoidal excitation of a passive element or system is

$$Q = 2\pi \frac{(peak.stored.energy)}{(energy.dissipated.per.cycle)} \tag{4.10}$$

For a second-order passive system, the two equations above are equivalent. We will see that Q has a simple interpretation in the Bode diagrams of second-order transfer functions.

We will find that Q (low pass filter) $\equiv R\sqrt{\frac{C}{L}}$ and transfer function of the low-pass filter is found to be:

$$\left|\frac{V_2(S)}{V_1(S)}\right| = \frac{1}{\sqrt{\left[1-\left(\frac{W}{W_0}\right)^2\right]^2 + \frac{(W/W_0)^2}{Q^2}}} \quad \text{For W} << W_0 : \ \frac{V_2}{V_1} = 1 \qquad (4.11)$$

$$\text{For W} >> W_0 : \ \frac{V_2}{V_1} \approx \left(\frac{W}{W_0}\right)^{-2} \qquad (4.12)$$

We plot this response including the resonant bump below. The resonant bump near $f = f_0$ is asymmetric in shape, and the transfer function is as shown in Eq. 4.13.

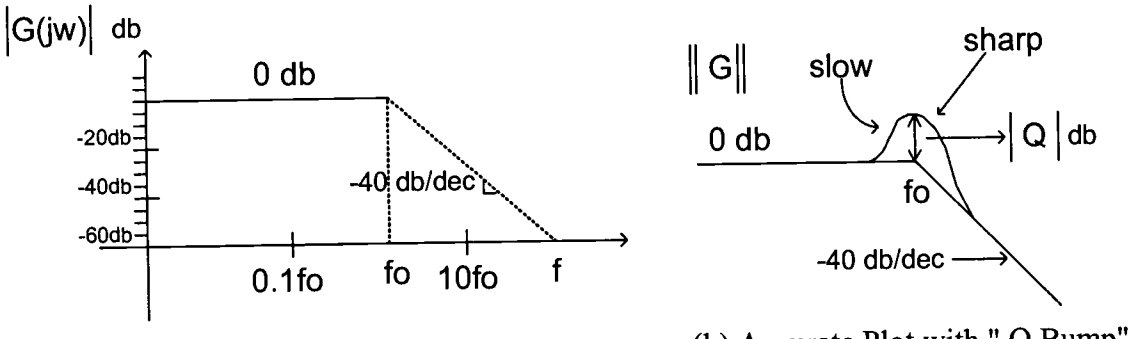

(a) Basic Plot

(b) Accurate Plot with " Q Bump"

Fig. 4.4 Basic Plot and Accurate Plot.

$$\frac{V_2(S)}{V_1(S)} = \frac{1}{1+\frac{L}{R}S+LCS^2} = \frac{1}{1+\frac{S}{Qw_0}+\frac{S^2}{W_0^2}} = \frac{1}{(1+S/W_1)(1+S/W_2)} \qquad (4.13)$$

Below we give the full-blown amplitude (with Q peaking) and phase plots for T(s) for the low-pass filter (Figs. 4.5 & 4.6).

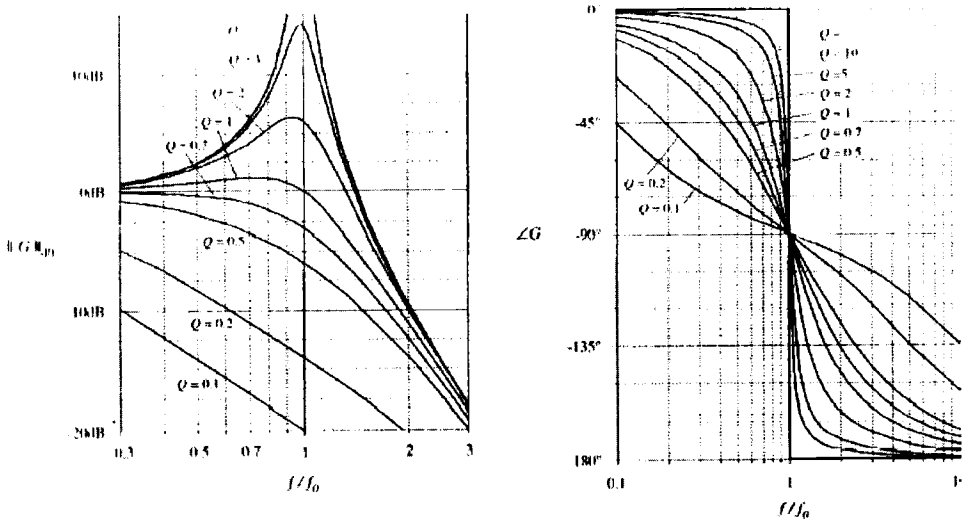

Fig. 4.5 The complete amplitude and phase plots.

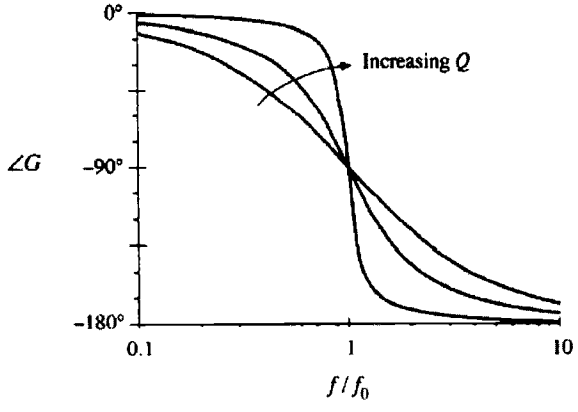

Fig. 4.6 Phase plot, second-order poles, Increasing Q causes a sharper phase change.

4.5 Selecting the Appropriate Filter Technology

The simplest low pass filter is the classic Butterworth pi network design where the reactive elements are of constant impedance. It exhibits the best low pass filter characteristics due to the following reasons.

1. Small number of elements but effective filter.
2. Economic and compact filter, which is low cost.
3. Low losses.
4. Minimum weight and space requirements.
5. Effective EMI filter.

The five major power filter technologies that can be considered within a low pass filter system for the flyback converter are:

1.Bessel

2. Butterworth

3.Chebyshev

4.Elliptic (Cauer)

5. Inverse Chebyshev

4.6 Typical Low Pass Filters

There are four key parameters that specify a low-pass filter as shown in Fig. 4.9: $f_{CUT\text{-}OFF}$, f_{STOP}, A_{MAX}, and M.

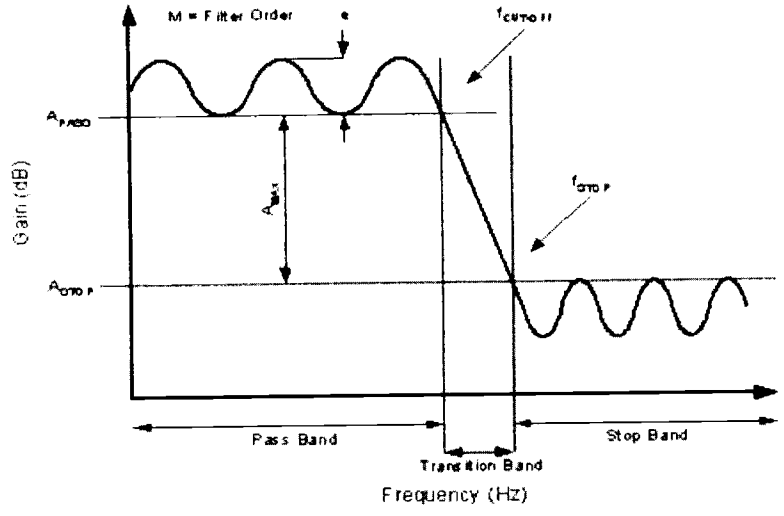

Fig. 4.7 The key low pass filter design parameters.

The cut-off frequency ($f_{CUT-OFF}$) of a low pass filter is normally defined as the -3dB point (e.g. Butterworth and Bessel filter) or the frequency at which the filter response leaves the error band (e.g. Chebyshev). Butterworth or Bessel filters do not create ripple in the pass band (i.e. flat) unlike the Chebyshev filter. The Chebyshev filter has a ripple up to the cut-off frequency, defined as ϵ. By definition, a low pass filter passes lower frequencies up to the cut-off frequency and attenuates the higher frequencies that are above the cut-off frequency. The filter order is determined by the number of poles in the transfer function (e.g. 3 poles, hence 3rd order). Generally, the greater number of poles a filter has the smaller the transition bandwidth. The Butterworth, Bessel, and Chebyshev are the three most popular filter designs. Other filter types that include inverse Chebyshev, Elliptic and Cauer designs are not used for output flyback converters. Detailed information on designing various types of filters including Butterworth and Chebyshev filter is presented in the next sections.

4.6.1 Butterworth Filter

The Butterworth filter is by far the most popular design used in circuits. This filter exhibits a monotonically decreasing transition with all the transition zeros at $\omega = \infty$, making it an all-pole filter. Therefore the transfer function of a Butterworth filter consists of all poles and no zeros and is equated to:

$$\frac{Vo}{Vin} = \frac{G}{a_0 s^n + a_1 s^{n-1} + a_2 s^{n-2} + \ldots a_{n-1} s^2 + a_n s + 1} \tag{4.17}$$

The frequency behavior has a maximally flat magnitude response in the pass-band. The rate of attenuation in the transition band is better than Bessel filter, but not as good as the Chebyshev filter. There is no ringing in the stop band, but there is some overshoot and ringing in the time domain, but less than the Chebyshev filter [22].

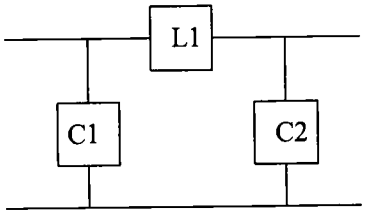

Fig. 4.8 Butterworth pi network low pass filter.

The attenuation of this particular filter is given by the equation:

$$A_{db} = 10\log\left[1 + \left(\frac{w}{w_C}\right)^{2n}\right]$$

w = The frequency of desired attenuation

w_C = The cutoff frequency (W_{3db}) of the filter

n = The number of elements in the filter

4.6.2 Chebyshev Filter

"The Chebyshev filter exhibits an equiripple response in the pass-band and a monotonically decreasing transmission in the stop-band. While the odd-order filter has |T(0)| = 1, the even-order filter exhibits its maximum magnitude deviation at $\omega = 0$. In both cases the total number of pass-band maxima and minima equals the order of the filter, N. All transmission zeros of the Chebyshev filter are at $\omega = \infty$, making it an all-pole filter [22]. Therefore, the transfer function of the Chebyshev filter is similar to the Butterworth filter in that it has all poles and no zeros with a transfer function of:

$$\frac{Vo}{Vin} = \frac{G}{a_0 + a_1 s + a_2 s^2 + \ldots a_{n-1} s^{n-1} + s_n} \tag{4.18}$$

4.7.3 Bessel Filter

The transfer function of the Bessel filter has only poles and no zeros. Where the Butterworth design is optimised for a maximally flat pass band response, the transition bandwidth, the Bessel filter produces a constant time delay with respect to frequency over a large range of frequencies. The transfer function for the Bessel filter is:

$$\frac{Vo}{Vin} = \frac{G}{a_0 + a_1 s + a_2 s^2 + \ldots a_{n-1} s^{n-1} + s_n} \tag{4.19}$$

The advantages of each filter type come at the expense of other characteristics. The Butterworth is considered by many to offer the best all-around filter response [22]. It has maximum flatness in the pass-band with moderate roll off past cutoff, and shows only slight overshoot in response to pulse input. The Bessel is important when signal-conditioning square-wave signals. The constant-group delay means that the square-wave signal is passed with minimum distortion (overshoot). This comes at the expense of a slower rate of attenuation above cutoff. The 3-dB Chebyshev sacrifices pass-band flatness for a high rate of attenuation near cutoff. Note that transfer function of Chebyshev and Bessel are the same but denominator coefficients for both designs are different.

Chapter 5

PROPOSED EFFICIENCY ENHANCEMENT MODIFICATION

5.1 Equal-Element Filter Improves Passband Performance

Filter designers originally conceived equal-element filters as all pole microwave bandpass filters that provide minimum center-frequency insertion losses for specific values of resonator-unloaded Q. All resonators of the equal-element bandpass filter operate at the same loaded Q [10].

For LC filters, the equal-element filter has another advantage. In the lowpass prototype, all inductors have the same value, and all capacitors have the same value. This minimum number of circuit elements provides design simplicity and reduces filter cost. However, the equal-element filter's response shape has one severe shortcoming. Passband amplitude ripples, due to reflection, are unacceptable for some applications. In minimum-phase-shift filter circuits, group-delay ripples that preclude equalization accompany the amplitude ripples. At microwave frequencies, modifying the central resonator of a five-pole bandpass filter leads to improved performance [10]. Fig.5.1 shows the schematic of a three-pole, equal-element, lowpass-filter prototype. Again, this is for medium-power (e.g. 40W) flyback converter output filters, which have been identified as having the greatest opportunity for hardware topology efficiency improvement for this thesis work.

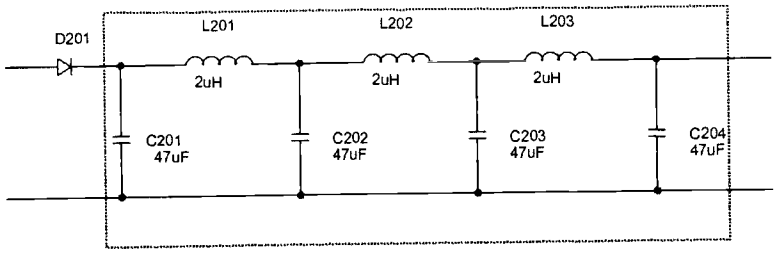

Fig. 5.1 Three stages of a three-pole equal-element filter.

5.2 Utilizing Higher LC order Stage

From the efficiency measurements in Chapter 3, we found that the converter efficiency will considerably increase if the output filters are upgraded to lower loss filters.

5.2.1 Single-stage LC filter for medium-power flyback converters

The circuit in Fig 5.2 is in the low-pass configuration. We shall measure the operation frequency, phase change, and the input and output power of the single-stage filter.

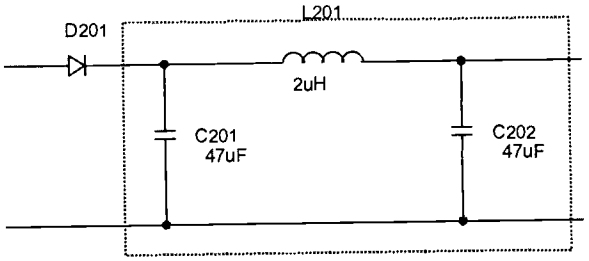

Fig. 5.2 Single-stage LC Filter.

For the single-stage circuit of Fig. 5.2, the roll-off rate is –20 dB/decade as seen in Fig. 5.3. The cut-off frequency at 3dB is 6.2711 kHz and the center frequency is 11.482 kHz.

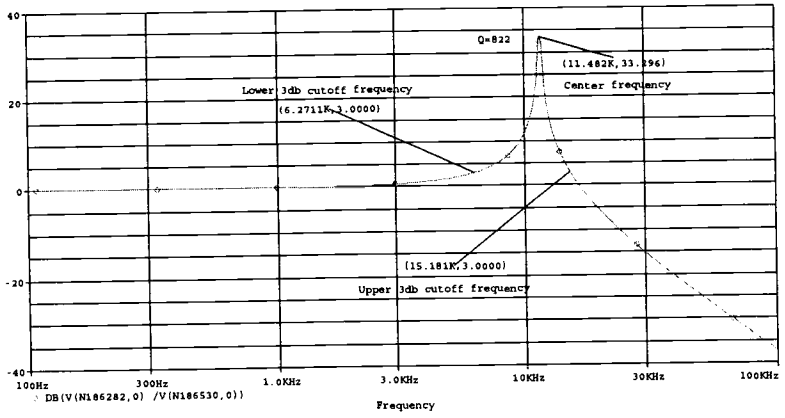

Fig. 5.3 DB plot versus frequency.

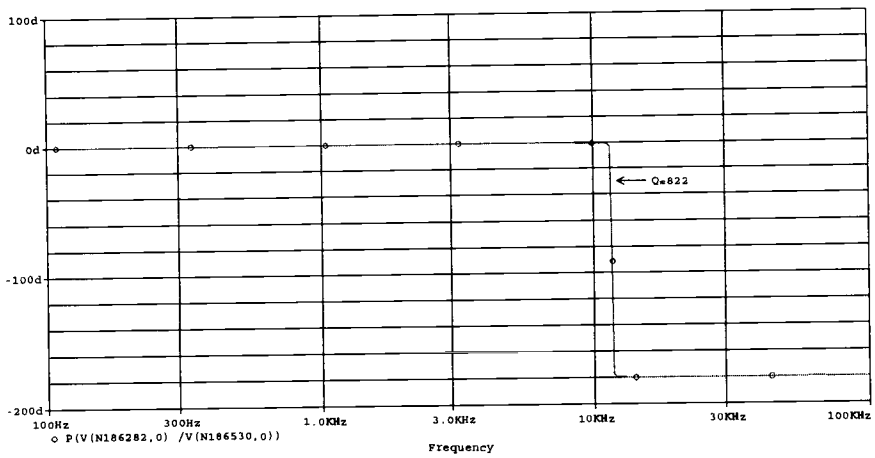

Fig. 5.4 Phase plot versus Frequency.

The trace of the phase angle in Fig. 5.4 shows that in the pass region of the filter, the phase angle changes abruptly from 0^0 to -180^0 since Q is high. From Fig. 5.5, we shall verify that the power at the input filter is distorted from the circuit. The RMS power from the input, measured at 150 milliseconds, is about 5.2818 (W), and the RMS power to the output is only about 4.0176 (W). Thus the ratio of power received to power delivered is 4.0176/5.2818, which is equal to 0.76, or about 76%. This is not so efficient a power transfer ratio. The next step is to investigate the two-stage filter to see any improvement in the power transfer ratio.

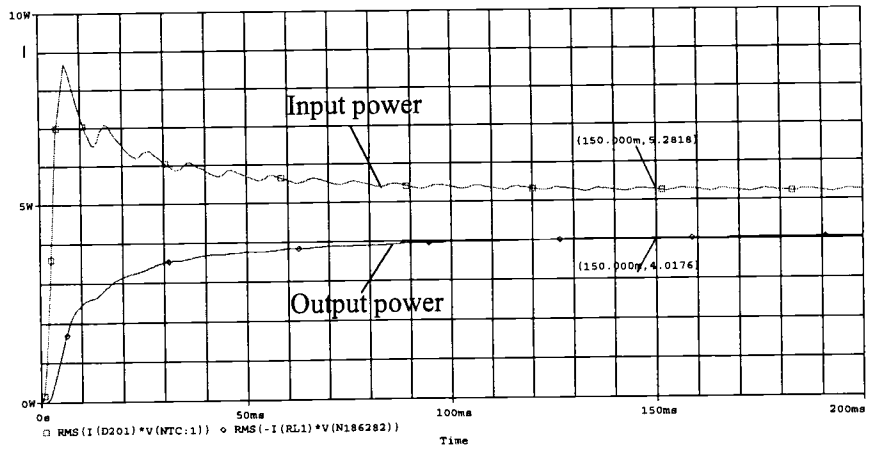

Fig. 5.5 Input and output power of a single-stage filter in the time domain.

5.2.2 Two-stage LC filter for medium-power flyback converters

We extend out investigation into filter circuits by adding an identical LC section to the circuit in Fig. 5.2 as is shown in Fig. 5.6. The two LC section need not be identical. Our objective is to find if there is any effect upon the roll-off rate and power delivered to the output from the input of this two-stage filter compared to the single-stage filter.

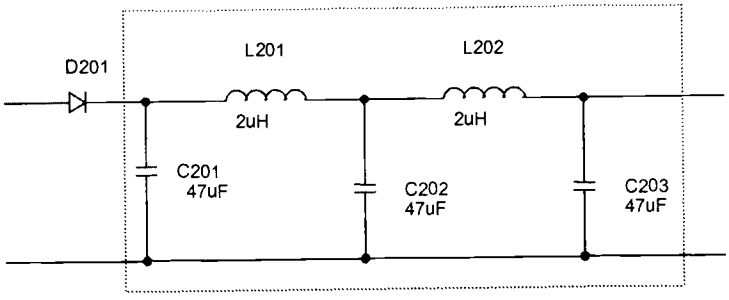

Fig. 5.6 Two-stage LC filter.

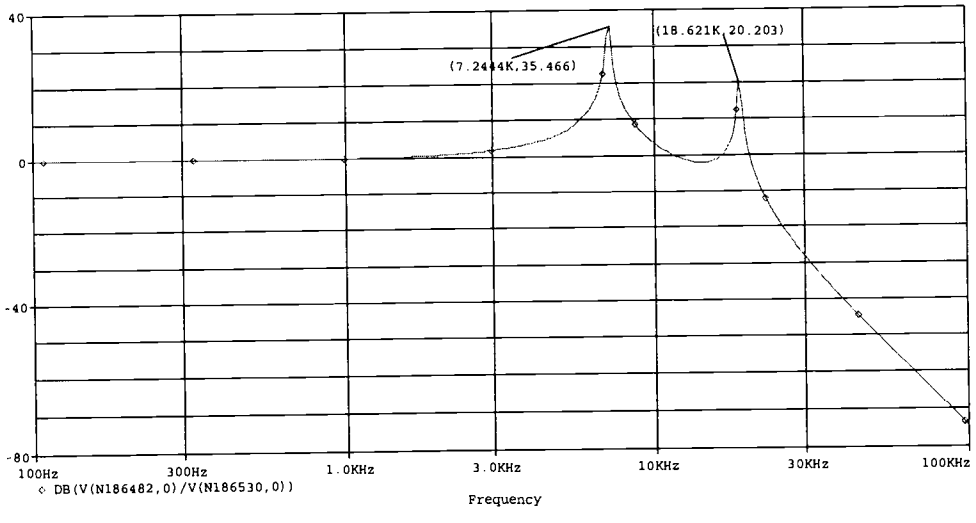

Fig. 5.7 DB plot versus Frequency.

From Fig. 5.7 we observe that the roll-off rate for the overall filter is steeper than that for the single-section filter. The logarithmic gain of the overall filter has changed by –40 dB/decade. This is double the rate for the single-stage filter. In practical terms this means that the two-stage filter discriminates more effectively against unwanted frequencies compared to the single-stage filter.

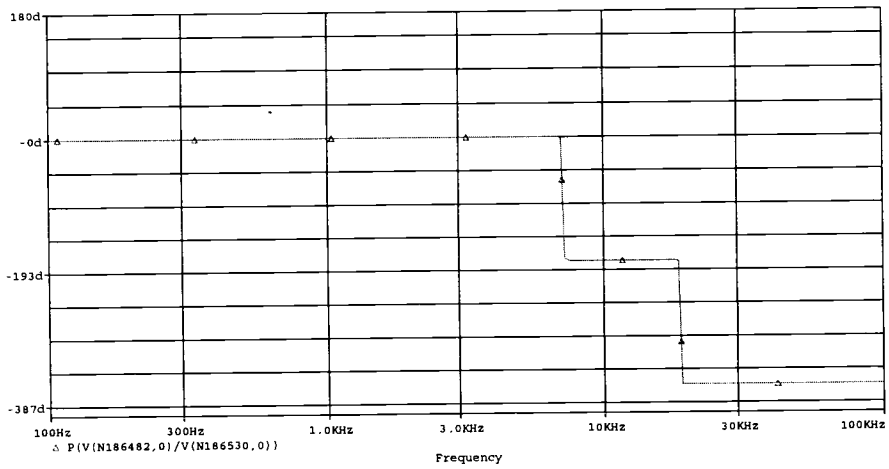

Fig. 5.8 Phase plot versus Frequency.

In Fig. 5.8 the trace of the phase angle shows that in the pass region of the filter, the phase angle changes abruptly from 0^0 to -360^0.

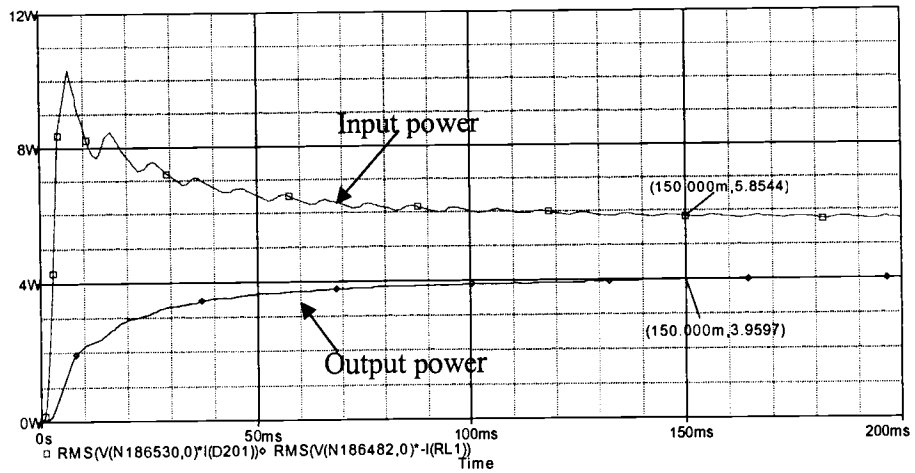

Fig. 5.9 Input and output power of a two-stage filter in the time domain.

The RMS power from the input in Fig. 5.9, measured at 150 (ms), is about 5.8544 watts, and the RMS power to the output is only about 3.9597 (W). Thus the ratio of power received to a power delivered is 3.9597/5.8544, which is equal to 0.676, or about 67.6%. This again is not an efficient power transfer ratio. We notice that the single-stage filter is more efficient than the two-stage filter in power transfer, but the two-stage filter is better in filtering frequency. The next step is to investigate the three-stage filter to see if there is any improvement in the power transfer ratio.

5.2.3 Three-stage LC filter for medium-power flyback converters

We extend out investigation into filter circuits by adding an identical LC section to the circuit in Fig. 5.6 as is shown in Fig. 5.10. The three LC sections need not be identical. Our objective is to find if there is any effect upon the roll-off rate and power efficiency delivered to the output from the input of this two-section filter compared to the single and two- section filter.

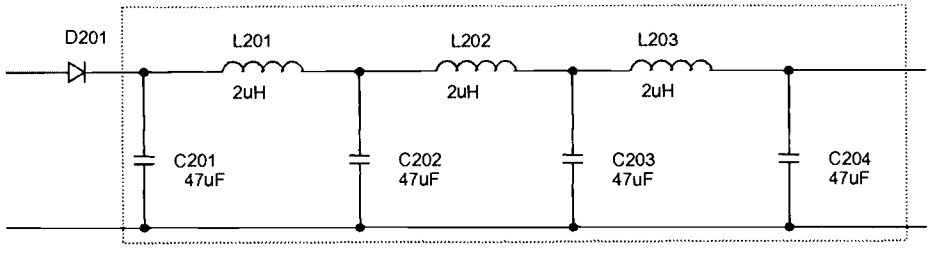

Fig. 5.10 Three-stage LC Filter.

From Fig. 5.11 we observe that the roll-off rate for the overall filter comprising the three identical LC sections is steeper than that rate for the single-section and two-section filter. The logarithmic gain of the overall filter has changed by –60 dB/decade. In practical terms this means that the triple-section filter discriminates more effectively against unwanted frequencies compared to the single-stage filter circuit.

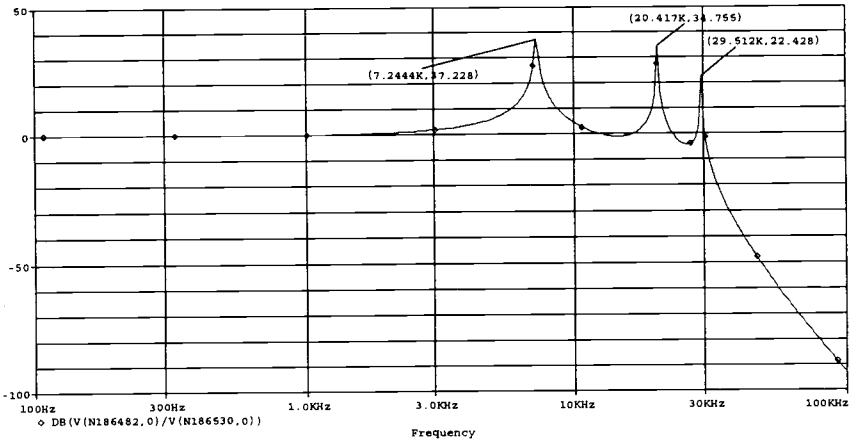

Fig. 5.11 DB plot versus Frequency.

In Fig. 5.12 the trace of the phase angle shows that in the pass region of the filter, the phase angle changes from 0^0 to -540^0.

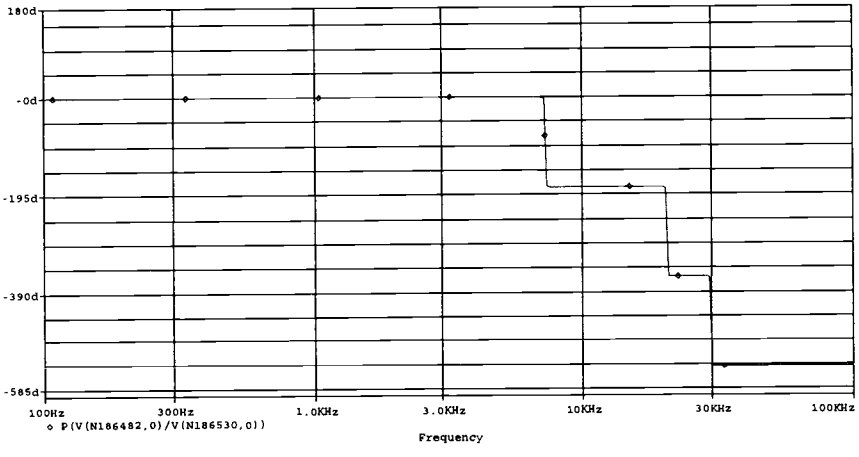

Fig. 5.12 Phase plot versus Frequency.

The RMS power from the input in Fig. 5.13, measured at 150 milliseconds, is about 6.333 watts, and the RMS power to the output is only about 3.9646 watts. Thus the ratio of power received to power delivered is 3.9646/6.333, which is equal to 0.626, or about 62.6%. This again is not an efficient power transfer ratio. We notice that the single-stage filter is more efficient than the two-stage and three-stage filter in power transfer, but the three-stage filter is better at eliminating unwanted frequencies.

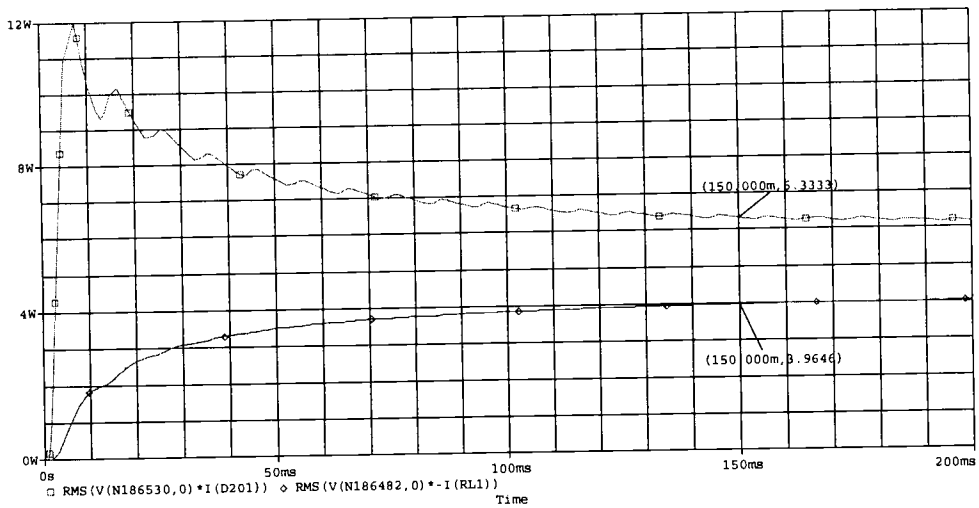

Fig. 5.13 Input and output power of three-stage filter in the time domain.

Then, we compare all three filters to see the different power transfer among them as shown in Fig 5.14. It is observed that adding the more stages of LC filter does not help in improving efficiency.

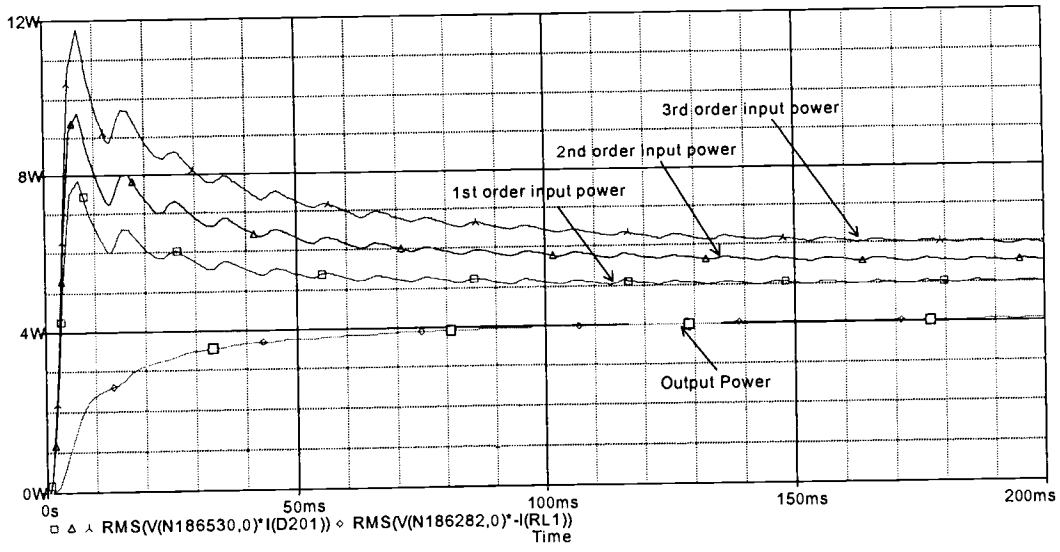

Fig. 5.14 The power comparison of three filters.

A next step is to investigate another approach by transforming the LC pi to a Double L network (T network filter) to see if the power transfer ratio could be improved. The double L network practically works well with low power and load impedance. We can transform Pi to T network as follows.

5.3 Transforming LC pi to Double L or T Networks

As the circuit theory, Pi filter network can be transformed to T network as follows.

5.3.1 Single- stage T filter for medium-power flyback converters

The circuit in Fig 5.15 (the single-stage T network configuration) is transformed from the single stage filter in Fig 5.2. We shall begin our investigation of the operation frequency, phase change, and the input and output power of the single-stage filter.

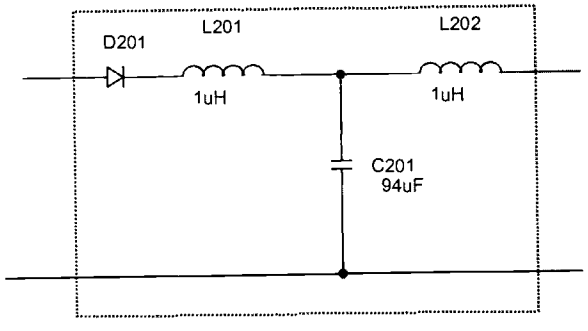

Fig. 5.15 Single-stage T network.

For the single-stage circuit of Fig. 5.15, the roll-off rate is –20 dB/decade as seen in Fig. 5.16. The cut-off frequency at 3dB is 6.2721 kHz and the center frequency is 11.482 kHz. Both the cut-off frequency and the center frequency are the same as the single-stage pi network.

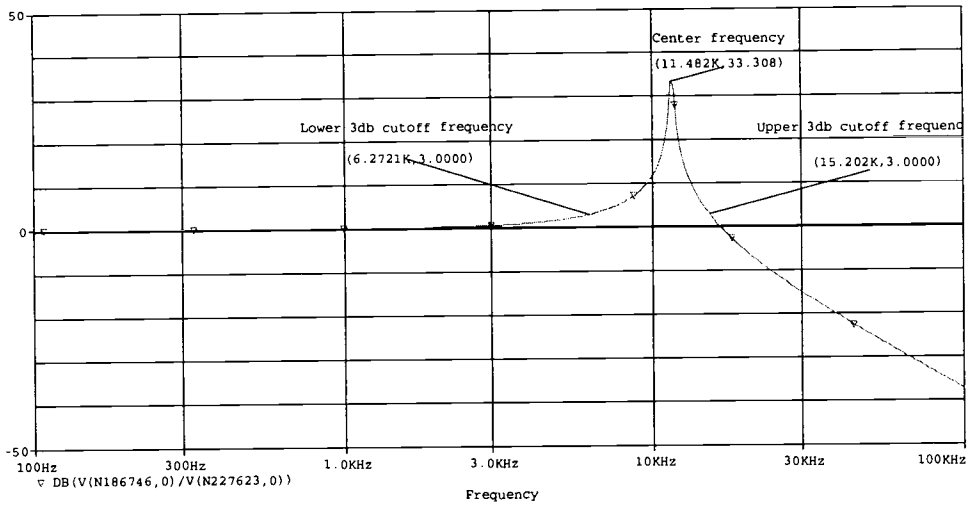

Fig. 5.16 DB plot versus Frequency.

In Fig. 5.17 the trace of the phase angle shows that in the pass region of the filter, the phase angle changes from 0^0 to -180^0.

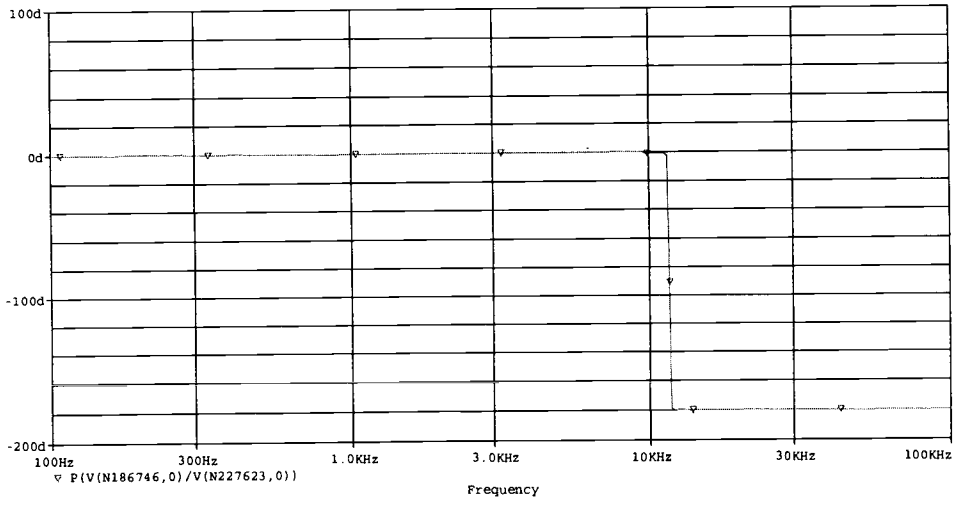

Fig. 5.17 Phase plot versus Frequency.

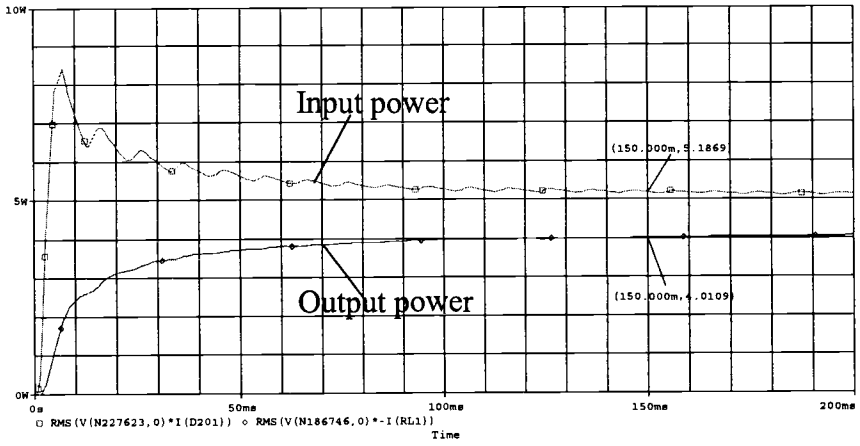

Fig. 5.18 Power input and output filter in the time domain.

From Fig. 5.18, The RMS power from the input, measured at 150 milliseconds, is about 5.1869 (W), and the RMS power to the output is only about 4.0109 (W). Thus the ratio of power received to power delivered is 4.0109/5.1869, which is equal to 0.773, or about 77.3%. We still need a better power transfer ratio. Next, we will investigate the two-stage filter to see if there is any improvement in the power transfer ratio.

5.3.2 Two-stage T filter for medium-power flyback converters

We next extend out investigation into filter circuits by adding an identical LC section to the circuit in Fig. 5.15 as is shown in Fig. 5.19. Our objective is to determine if there is any effect upon the roll-off rate, the phase angle of the output, and average power delivered to the output from the input of this two-stage filter compared to the single-stage filter.

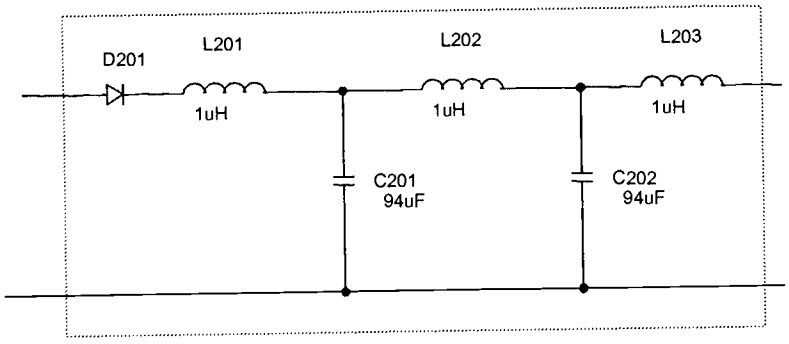

Fig. 5.19 Two-stage T network filter.

From Fig 5.20 we observe that the roll-off rate for the overall filter is steeper than that rate for the single-stage filter. The logarithmic gain of the overall filter has changed by –40 dB/decade. This is double the rate for the single-stage filter. In practical terms this means that the two-stage filter discriminates more effectively against unwanted frequencies compared to the single-stage filter circuit exactly like the two-stage pi network.

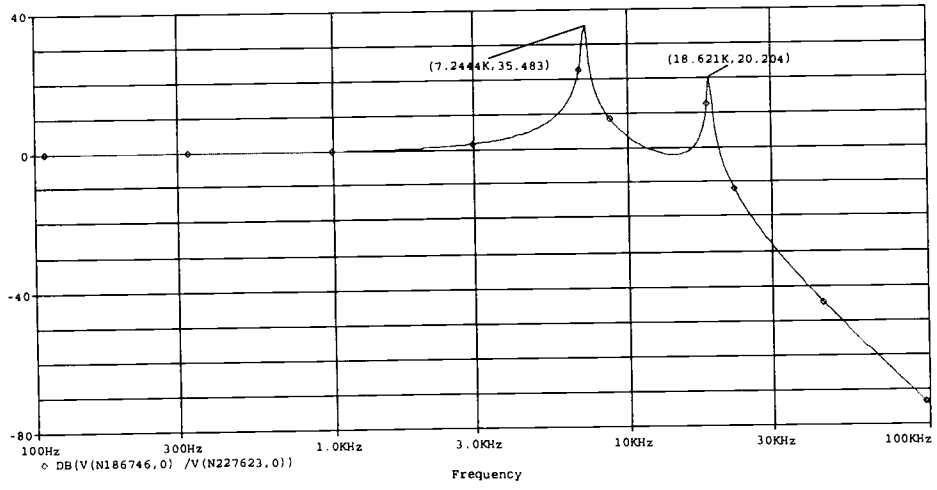

Fig. 5.20 DB plot versus Frequency.

In Fig. 5.21 the trace of the phase angle shows that in the pass region of the filter, the phase angle changes abruptly from 0^0 to -360^0.

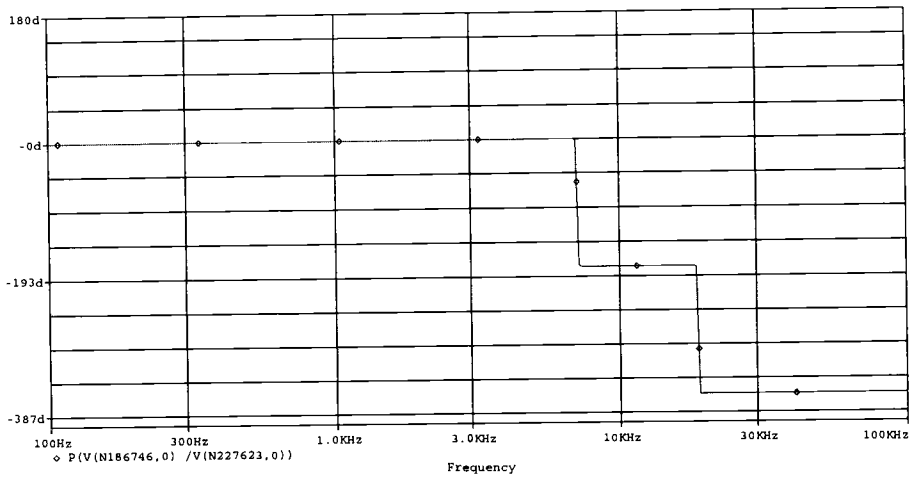

Fig. 5.21 Phase plot versus Frequency.

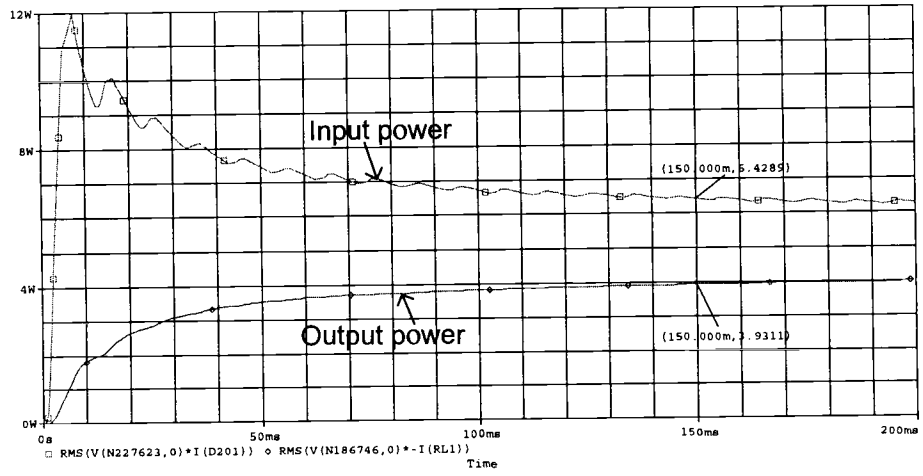

Fig. 5.22 Power input and output filter in the time domain.

The RMS power from the input in Fig. 5.22, measured at 150 (ms), is about 6.4289 (W), and the RMS power to the output is only about 3.9311 (W). Thus the ratio of power received to power delivered is 3.9311/6.4289, which is equal to 0.611, or about 61.1%. We notice that the single-stage filter is more efficient than the two-stage filter in power transfer, but the two-stage filter is better in filtering frequency. In addition, we can estimate that the three-stage of T network will operate the same as that of pi network.

Also, we compare all three filters in parallel to see the different power transfer among them as shown in Fig 5.23. It can be observed that there is no improved efficiency by adding the more stages of LC filter.

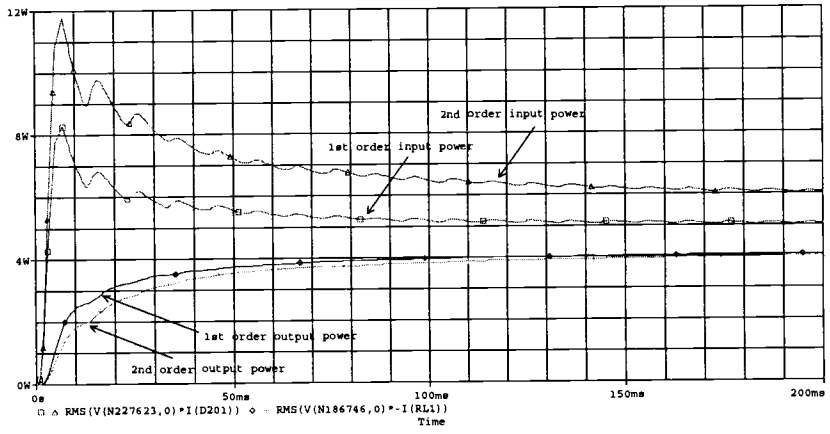

Fig. 5.23 The power comparison of one and two-stage T filter.

We shall next analyze the effective of optimizing the filter LC parameters.

5.4 Optimizing L and C parameters

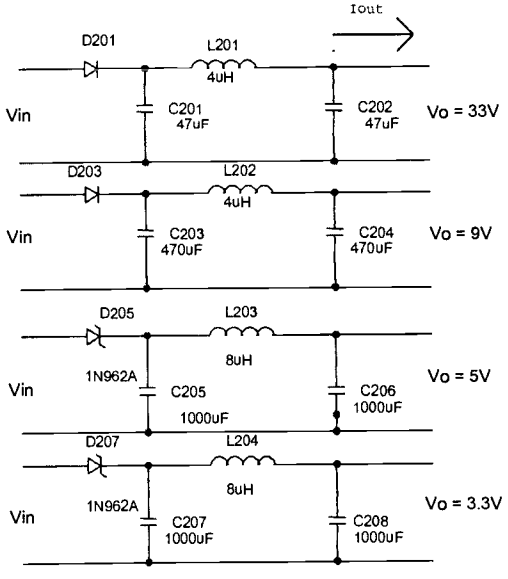

Fig. 5.24 Output stage.

5.4.1 Selection of Output Power Inductors

(A) General Considerations

Most switching power supply designs use an inductor as part of the output-filtering configuration. The presence of this inductor is two-fold: first it stores energy during the off or "notch" periods in order to keep the output current flowing continuously to the load, and second it aids to smooth out and average the output voltage ripple to acceptable levels.There are a variety of cores that we use in the design of inductors. The most popular materials used in present-day high-frequency switching designs are ferrite cores, iron powder cores, and molypermalloy (MPP) cores. All of these cores are good for power inductor designs, and basically the criterion of choosing one vs. the other is based on factors such as cost, weight, availability, performance, and ease of manufacture. Iron powder and MPP cores are generally offered in toroid forms, and they are well suited for power chokes because of the following characteristics:

1. High saturation flux density (Bsat) up to 8000 G.
2. High-energy storage capability.
3. Inherent air gap eliminates the need of gapping the core.
4. Wide choice of sizes.

Ferrite cores, on the other hand, have to be gapped because of their low saturation flux density (Bsat), they are more temperature sensitive, and they tend to be bulkier. But if pot cores are used for output chokes, radiated EMI will be reduced because of the inherent shielding properties of the pot core. Also, ferrite chokes are easier to wind, especially if heavy-gauge wire is involved [1].

(B) Deriving the Design Equations

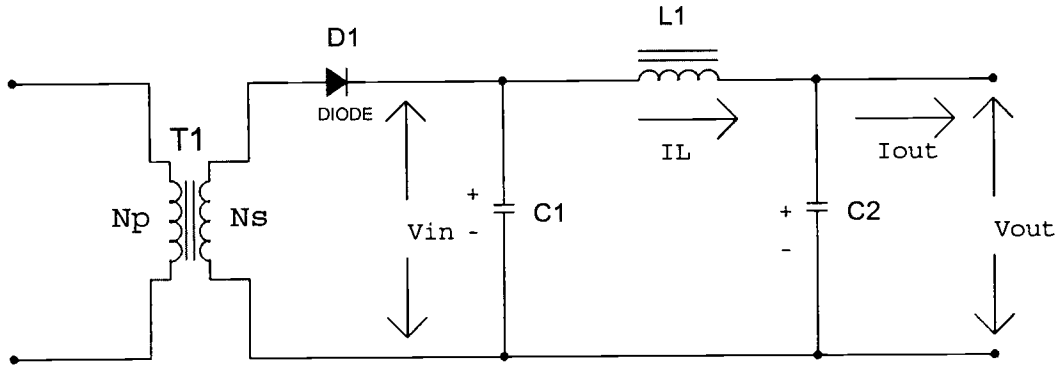

Fig. 5.25 The output section of a PWM flyback converter.

Consider the output section of a PWM flyback converter depicted in Fig. 5.25. From basic electrical theory, the voltage across the inductor is given by

$$V_L = L\frac{di}{dt} \tag{5.1}$$

Since

$$V_L = Vin - Vout \tag{5.2}$$

And

$$di = \Delta I_L$$

then Eq. 5.1 may be written, solving for L, as follows;

$$L = \frac{[Vin - Vout] \times \Delta t}{\Delta I_L} \tag{5.3}$$

In order to keep low inductor peak current and good output ripple, it is recommended that ΔI_L should be about 0.25 I_{out} [10].

Based on this Eq.5.1 may be rewritten as follows:

$$L = \frac{[Vin - Vout] \times Toff}{0.25 I_{out}} \tag{5.4}$$

V_{out} = the output voltage

V_{in} = the highest peak voltage following the output rectifier of that particular output

T_{off} = the estimated on time of power switches at the highest input voltage (30 percent of 1/f)

I_{out} = the highest expected load current for that output.

We can estimate *Vin* and *Vout* from Table 2, and the rated inductor currents are (see Fig 1.7):

I_{L201} = 0.1 A

I_{L202} = 0.5 A

I_{L203} = 1.2 A

I_{L204} = 1.5 A

In order to keep the inductance low and an acceptable output ripple for the highest voltage, it is recommended that ΔI_L should be approximately $2.5I_{out}$ [10]. Then the inductor values are calculated to be:

$$L_{201} = \frac{0.46 \times \frac{0.3}{70000}}{2.5 \times 0.1} = 7.88 \text{ uH} \approx 8 \text{ uH}$$

$$L_{202} = \frac{0.244 \times \frac{0.3}{70000}}{0.25 \times 0.5} = 8.36 \text{ uH} \approx 8 \text{ uH}$$

$$L_{203} = \frac{0.277 \times \frac{0.3}{70000}}{0.25 \times 1.2} = 3.9 \text{ uH} \approx 4 \text{ uH}$$

$$L_{204} = \frac{0.117 \times \frac{0.3}{70000}}{0.25 \times 1.5} = 1.34 \text{ uH} \approx 2 \text{ uH}$$

Optimization of the L and C parameters also requires analyses and verification of the resulting output ripple which will be addressed in Section 5.4.4, as well as in Chapter 6 in the experimental results.

5.4.2 Output Capacitor Requirements

The output capacitors in switched-mode power supplies perform the functions of energy storage and filtering. The storage of energy calls for very high capacitances. The capacitors have considerable ohmic and inductive components at the high frequencies used. The capacitors employed in high-current switched-mode power supplies may have a very low resistance R_c, i.e. an equivalent series resistance (ESR) is equal to a few milliohms. The same applies to inductance L_c, i.e. the equivalent series inductance (ESL). Capacitors with a maximum of 5 nH inductance should be employed preferably.

5.4.3 Selection of Output-Filter Capacitors

Typically, the output capacitors used in switching regulators are large, must operate at high frequencies and require low ESR and equivalent series inductance (ESL). A good trade-off between cost and performance is the solid-tantalum capacitor, constructed of sintered tantalum powder particles packed around a tantalum anode, which makes a rigid assembly or slug. Compared to aluminum electrolytic capacitors, solid-tantalum capacitors have a higher capacity-voltage (CV) product per-unit volume, are more stable, and have hermetic seals to eliminate the effects of humidity. Next, we will calculate capacitor values for our filters

f_C = the desired cut-off frequency ($10\,kHz$)

A) Calculation for $C_{201,202}$ and $C_{203,204}$

$w = 2\pi f$

From section 5.4.1, the calculated inductor values for output voltage of 9V and 33V are $8\,uH$

$$X_L = wL$$
$$= 2\pi f_C L$$
$$= 2\pi \times 10 \times 10^3 \times 8 \times 10^{-6}$$
$$= 0.5\,\Omega$$

$X_L = X_C$

$$C_{201,202} = \frac{1}{2\pi f_C X_C}$$
$$= \frac{1}{2\pi \times 10 \times 10^3 \times 0.5}$$
$$= 30\ uF$$

Available capacitor value is $33\ uF$ and we consider that C is large enough not to cause output voltage ripple.

$C_{201,202} = C_{203,204}$

B.) Calculation for $C_{205,206}$

Calculated inductor value for output voltage of 5V is $4\,uH$

$$X_L = 2\pi f_C L$$
$$= 2\pi \times 10 \times 10^3 \times 4 \times 10^{-6}$$
$$= 0.2513\,\Omega$$

$$C_{205,206} = \frac{1}{2\pi f_C X_C}$$
$$= \frac{1}{2\pi \times 10 \times 10^3 \times 0.2513}$$
$$= 63\ uF$$

Available capacitor value is 100 uF and we consider that C is large enough not to cause output voltage ripple.

C.) Calculation for $C_{207,208}$

Calculated inductor value for output voltage of 3.3V is $2\,uH$

$$X_L = 2\pi f_C L$$
$$= 2\pi \times 10 \times 10^3 \times 2 \times 10^{-6}$$
$$= 0.12566\,\Omega$$

$$C_{207,208} = \frac{1}{2\pi f_C X_C}$$
$$= \frac{1}{2\pi \times 10 \times 10^3 \times 0.12566}$$
$$= 126.6\ uF$$

Available capacitor value is 180 uF and we consider our assumption that C is large enough not to cause output voltage ripple.

5.4.4 Ripple Considerations

Optimization of the output filter L and C parameters requires analyses of the output ripple. The output voltage ripple should be limited to 1% - 2% [1] depending on the application requirements. Output ripple voltage is a small triangular ac waveform that rides atop the dc output voltage [1]. To calculate the value of the output ripple we execute Eq. 5.5 using the optimized parameters.

$$V_{ripple(pk-pk)} = \frac{I_{out} \times D_{\min}}{f \times C_{out}} \tag{5.5}$$

$$\%V_{ripple(pk-pk)} = \frac{V_{ripple(pk-pk)}}{V_{out}} \times 100 \tag{5.6}$$

I_{out} = the rated output current for that output.

V_{out} = the rated output voltage for that output.

D_{min} = the smallest estimated duty cycle (0.3)

$V_{ripple(pk-pk)}$ = allowable peak-to-peak output voltage ripple (1 percent of the direct output voltage V_{out}).

f = switching frequency (this power switch = 70kHz)

Again, the rated output currents for the medium-power (40W) flyback converter are:

I_{L201} = 0.1 A I_{L202} = 0.5 A

I_{L203} = 1.2 A I_{L204} = 1.5 A

A.) Calculation of the output voltage ripple at 33V output

$$V_{ripple(pk-pk)} = \frac{0.1 \times 0.3}{70 \times 10^3 \times 33 \times 10^{-6}} = 0.013$$

$$\%V_{ripple(pk-pk)} = \frac{0.013}{33} \times 100 = 0.04\%$$

B.) Calculation of the output voltage ripple at 9Voutput

$$V_{ripple(pk-pk)} = \frac{0.5 \times 0.3}{70 \times 10^3 \times 33 \times 10^{-6}} = 0.06$$

$$\%V_{ripple(pk-pk)} = \frac{0.06}{9} \times 100 = 0.6\%$$

C.) Calculation of the output voltage ripple at 5Voutput

$$V_{ripple(pk-pk)} = \frac{1.2 \times 0.3}{70 \times 10^3 \times 100 \times 10^{-6}} = 0.05$$

$$\%V_{ripple(pk-pk)} = \frac{0.05}{5} \times 100 = 1\%$$

D.) Calculation of the output voltage ripple at 3.3Voutput

$$V_{ripple(pk-pk)} = \frac{1.5 \times 0.3}{70 \times 10^{3} \times 180 \times 10^{-6}} = 0.035$$

$$\%V_{ripple(pk-pk)} = \frac{0.035}{3.3} \times 100 = 1.06\%$$

As shown above, the optimized parameters did limit the output voltage ripple to 1% or less for output voltages of 33V, 9V, 5V&3.3V, and slightly greater (1.06%) for the 3.3V output.

5.4.5 Simulation

A) Output filter of 33V

Based on the calculation above, we apply the inductance and capacitance values to our circuit in Fig. 5.24. First, simulation shows the DB plot versus frequency in Fig. 5.26. The roll-off rate is –20 dB/decade. The cut-off frequency at 3dB is 7.0281 kHz and the center frequency is 12.883 kHz. The capability of filtering is the same as a single-stage of pi and T network approaches investigated earlier.

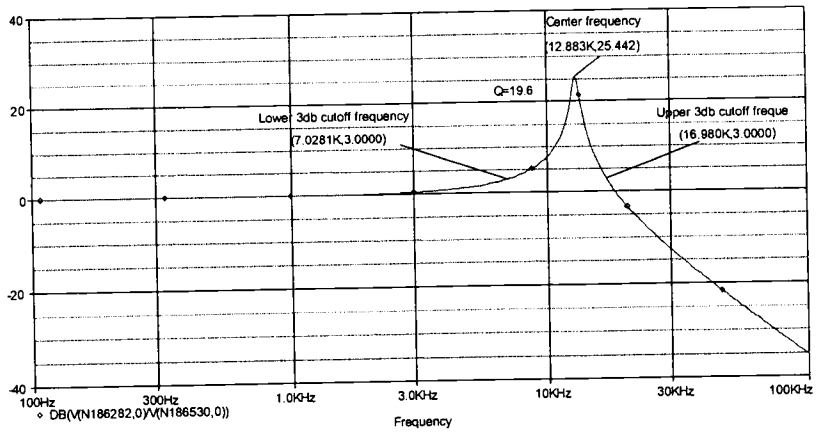

Fig. 5.26 DB plot versus Frequency.

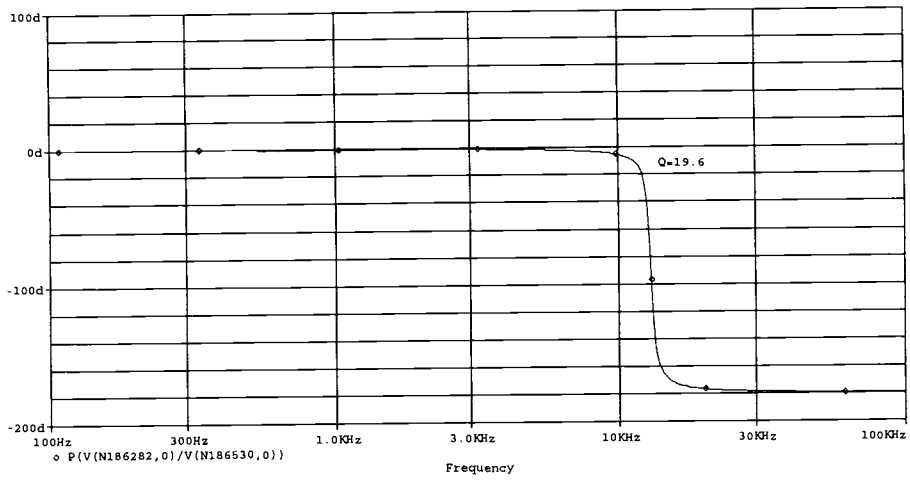

Fig. 5.27 Phase plot versus Frequency.

The trace of the phase angle in Fig. 5.27 shows that in the pass region of the filter, the phase angle changes abruptly from 0^0 to -180^0. The phase angle is not as steep as that for the earlier approaches.

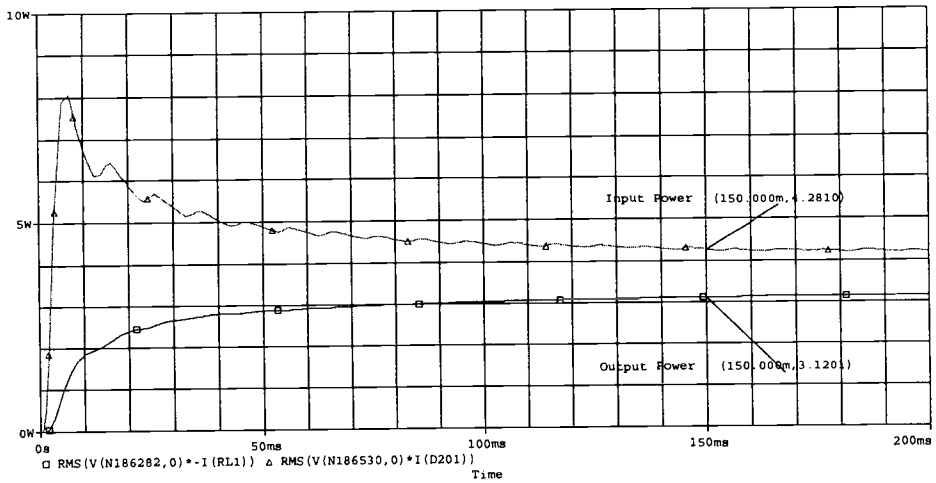

(a) Input and output power before modification.

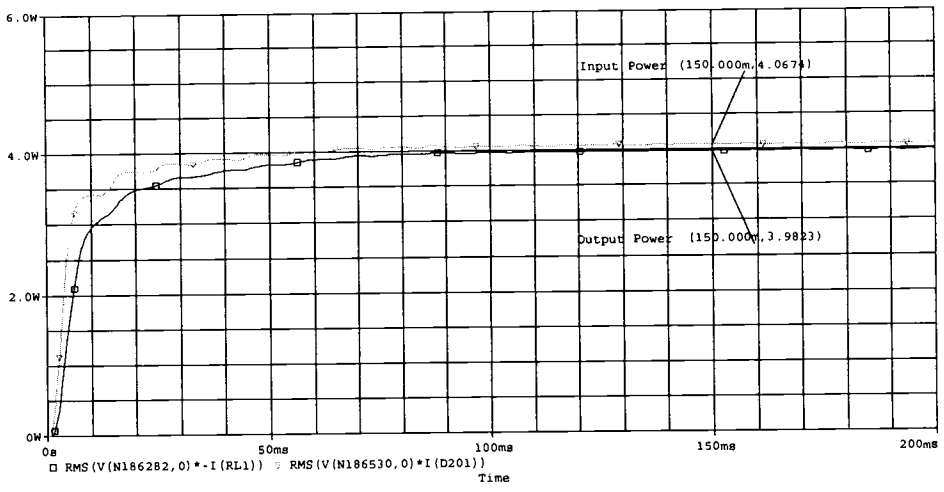

(b) Input and output power after modification.

Fig. 5.28 Input and output power in the time domain before and after modification.

Fig.5.28 above shows the efficient filter, which transfers input power to the output at almost no loss. We can see roughly the same power measured at 150 (ms). This is the goal filter that we are looking for. The result makes it possible to reduce the secondary isolated transformer coils, which mean reduced transformer size and cost. Finally we will gain improved efficiency, from 72.9% before the proposed parameter modification to 97.9% after the proposed implementation.

B) Output filter of 9V

The next step is to simulate the output filter at 9V and we will focus only on the power transfer or any efficiency improvement by comparing before and after modification as shown in Fig. 5.29.

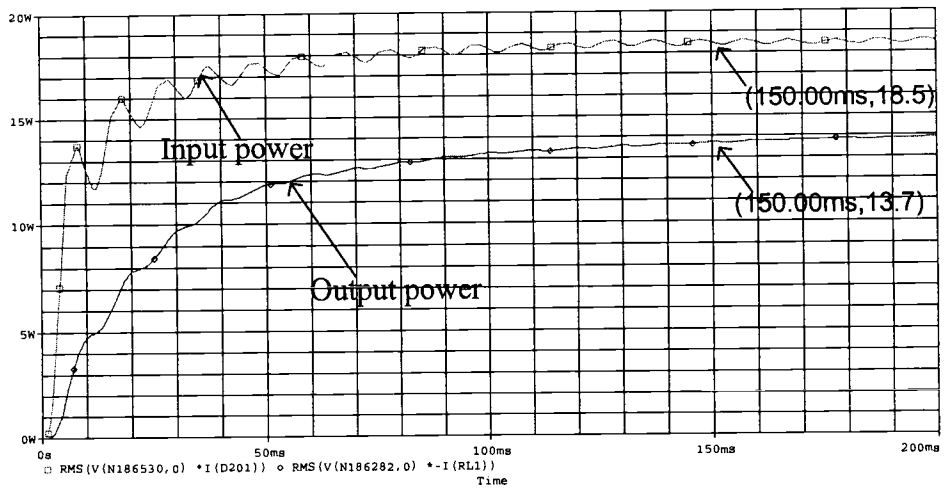

(a) Input and output power before adjustment.

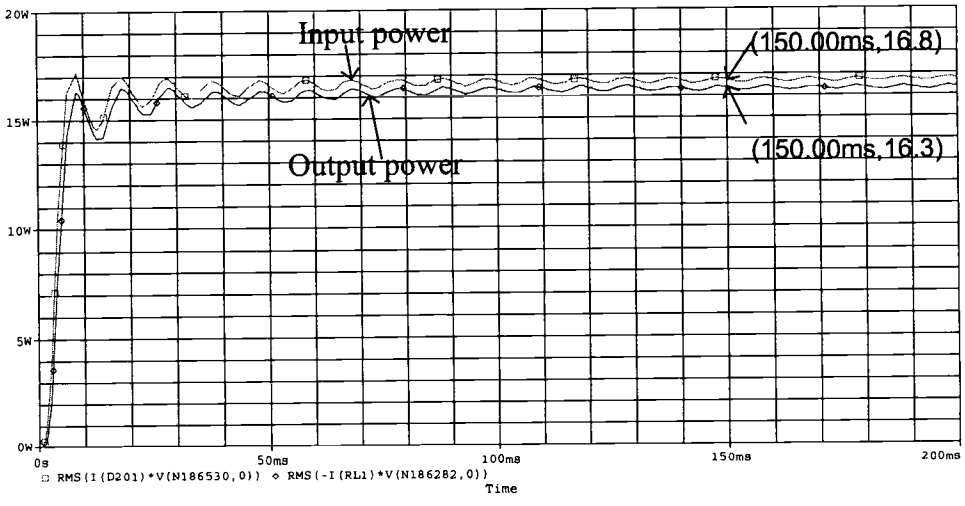

(b) Input and output power after modification.

Fig. 5.29 Input and output power with C = 33uF, L= 8uH after modification.

The difference between the input and output power in (a) and (b) clearly demonstrate the improved efficiency of the power transfer after modifying the LC filters; an improvement from 74.1% efficient to 97%.

C) Output filter of 5V

We shall apply the same method as before with the output filter of 5V and see the results illustrated in Fig. 5.30.

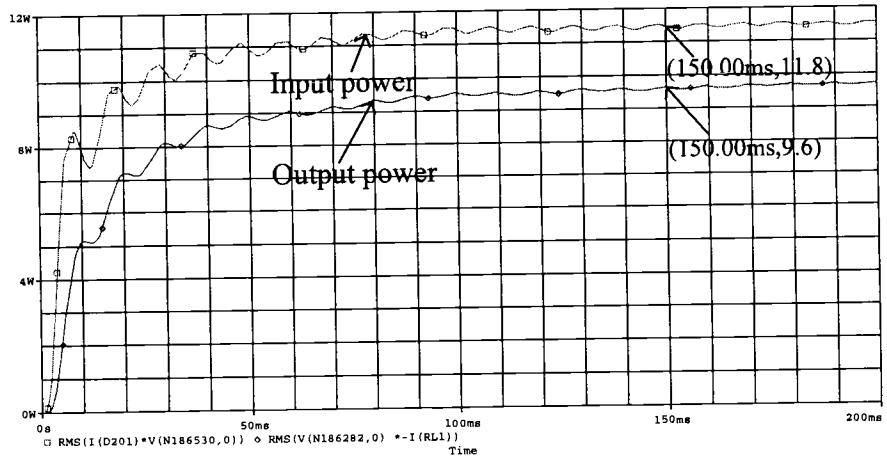

(a) Input and output power before adjustment.

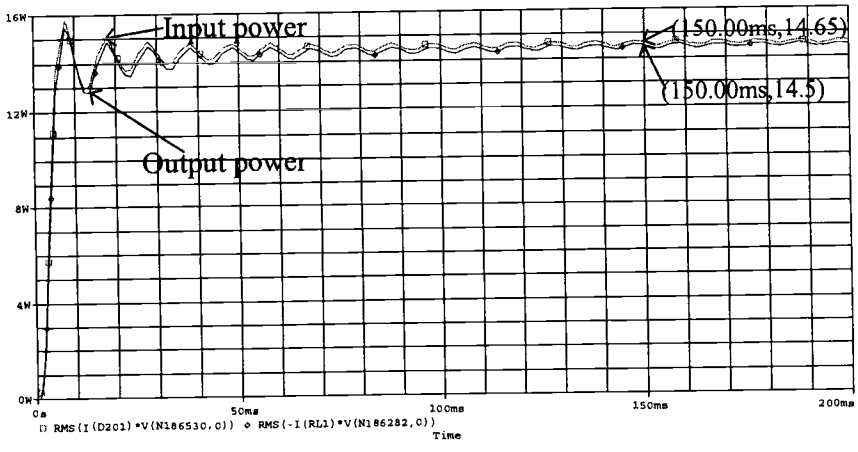

(b) Input and output power after adjustment

Fig. 5.30 Input and output power with C = 100uF, L= 4uH after modification.

Again we see the efficiency improvement from the output filter in (a) compared to (b) with a respective efficiency improvement of 81.3% to 98.9%

D) Output filter of 3.3V

Finally, we will simulate at the output filter of 3.3V. The results are illustrated in Fig. 5.31.

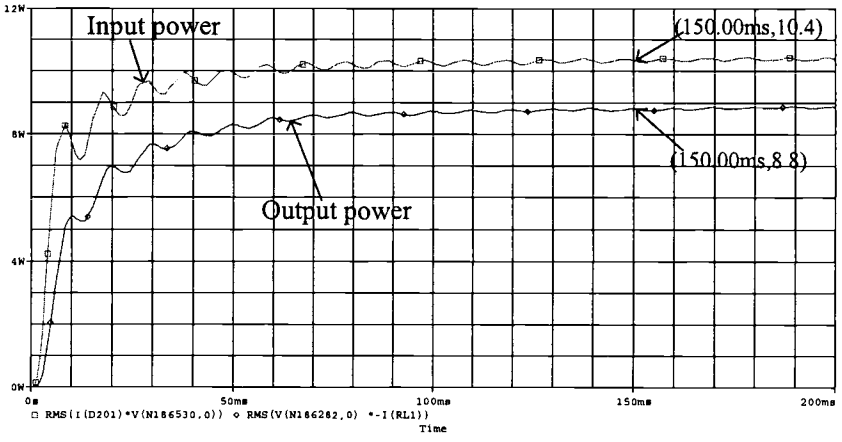

(a) Input and output power before adjustment.

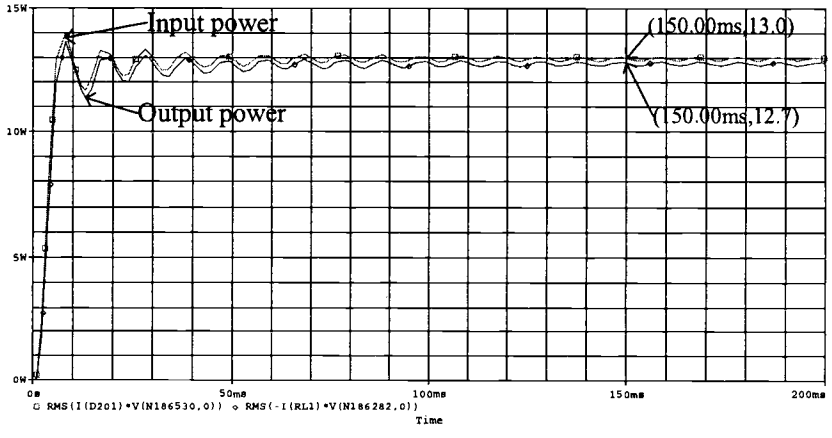

(b) Input and output power after adjustment.

Fig. 5.31 Input and output power with C = 180uF, L= 2uH after modification.

Again our approach is evident for the improved efficiency of the output filter, an improvement of 84.6% to 97.7%, all calculated parameters theoretically work well with the output filter. Subsequently, we shall apply our approach practically to the hardware medium-power flyback converter in Chapter 6.

Chapter 6

EXPERIMENTAL RESULTS OF EFFICIENCY ENHANCEMENT MODIFICATION

The primary efficiency improvement target from Table 3 of the medium-power flyback converter is the output filter. After investigating various approaches, optimization of the inductor and capacitor parameters has been determined to be a successful efficiency improving approach. If the losses in the output filter could be virtually eliminated, the total converter efficiency could be improved from 57.8% to 89% as shown below.

Input power = 33.78 W

Output power = 30.12 W

$$\text{Efficiency} = \frac{30.12}{33.78} \times 100 = 89\%$$

Fig. 6.1 shows the medium-power flyback converter with the original LC values and the optimized values.

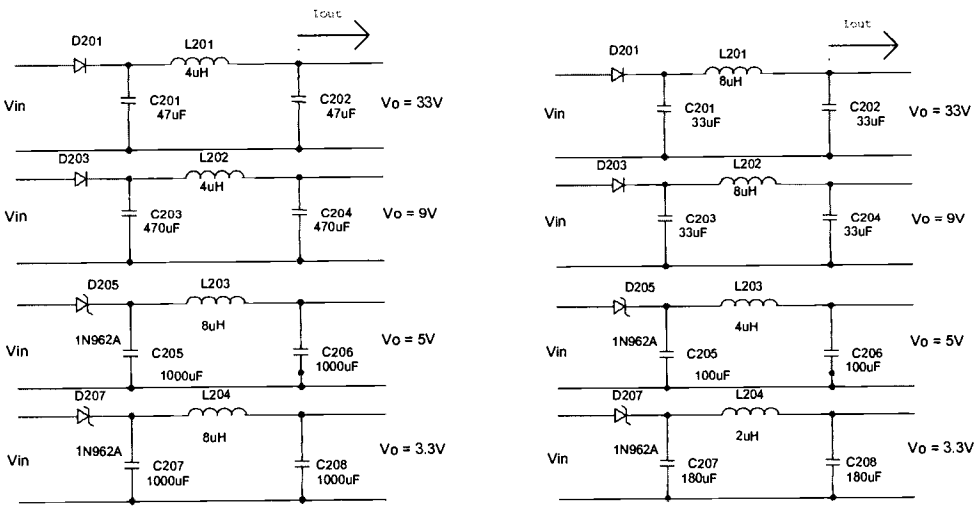

(a) The original LC values (b) The optimized LC values

Fig. 6.1 The medium-power flyback filter with the original and optimized values.

The results after applying the optimized LC parameters are as follows.

The input voltage and current waveforms with the optimized parameters of the converter are shown in Fig. 6.2. The total converter input power is 34.02W. The total output power is the sum of the 33V, 9V, 5V& 3.3V output power.

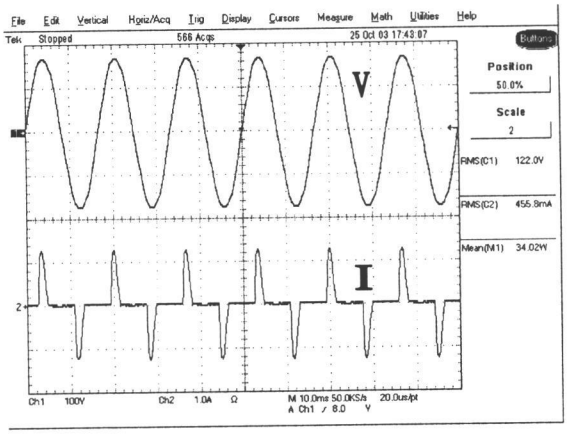

Fig. 6.2 Input waveforms.

The 33V-output filter results in Fig. 6.3 show the output voltage and current waveforms smoothed as dc and the output power is 9.17W. The output voltage ripple is measured to be 0.8%, This is larger than the theoretical ripple of 0.04% due to the experimental hardware parameter variations.

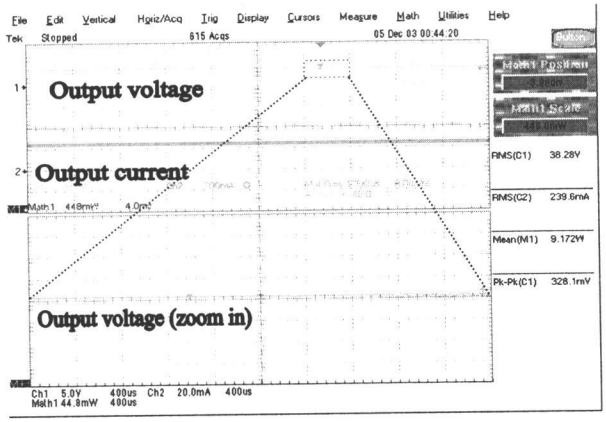

Fig. 6.3 33V output.

The 9V output filter results in Fig. 6.4 show the output voltage and current waveforms smoothed as dc and the output power is 6.082W. The output voltage ripple is 1.5%, which again is larger than theoretical as discussed in the 33V output case. The targeted applications would need to allow a 1.5% output voltage ripple.

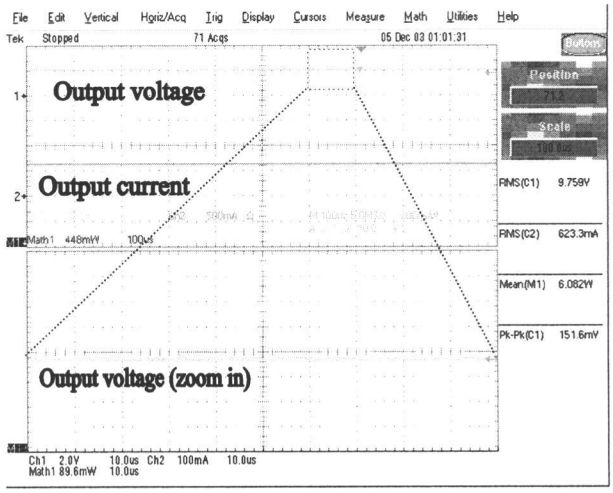

Fig. 6.4 9V output.

The 5V output filter results in Fig. 6.5 show the output voltage and current waveforms smoothed down as dc and the output power is 9.632W. The voltage ripple is 0.9%, which matches well with the theoretical calculation of 1%.

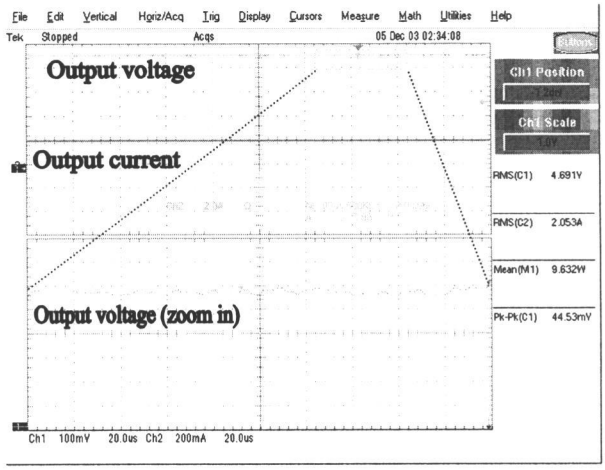

Fig. 6.5 5V output.

The 3.3V output filter results in Fig. 6.6 shows the output voltage and current waveforms smoothed as dc and the output power is 3.571W. The output voltage ripple is 1.7%, which again is larger than theoretical as discussed in the 33V output case. The targeted applications would need to allow a 1.7% output voltage ripple.

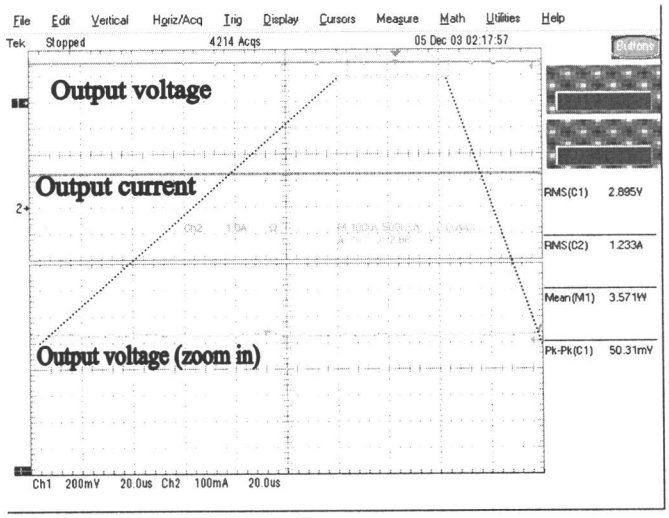

Fig. 6.6 3.3V output.

Table 5. Input and Output measurement after modification

Position	Vrms (V)	Irms (A)	P (W)	PF
Input	122	0.4558	34.02	0.612
Output (33V/0.1A)	38.28	0.239	9.17	1
Output (9V/0.5A)	9.759	0.623	6.082	1
Output (5V/1.5A)	4.691	2.053	9.632	1
Output (3.3V/1.2A)	2.895	1.233	3.571	1

Now all input and output powers are tabulated in Table 5. From the table we shall determine the final efficiency as follows.

The input power is

Pin = 34.02 W

The output power is

Pout = 9.17+ 6.082+ 9.632+ 3.571= 28.455 W

The power loss is

Ploss = 34.02-28.455 = 5.56 W.

The whole efficiency is

Efficiency = 28.455 / 34.02 = 83.6%

The final efficiency is 83.6 %; a substantial improvement over the original 57.8%. The overall efficiency improvement is on the order of a 25.8% improvement. The table summary of original and modified components and resulting efficiency improvement are shown below.

Table 6 Original and modified components and resulting efficiency improvement

	$C_{201,202}$	$C_{203,204}$	$C_{205,206}$	$C_{207,208}$	L_{201}	L_{202}	L_{203}	L_{204}	Efficiency
Original components	47uF	470uF	1000uF	1000uF	2uH	4uH	8uH	8uH	57.8%
Modified components	33uF	33uF	100uF	180uF	8uH	8uH	4uH	2uH	83.6%

Chapter 7

CONCLUSIONS AND RECOMMENDATION FOR FUTURE WORK

Ideally, the output of most power supplies should be a constant voltage. Unfortunately, this is difficult to achieve. There are two factors that can cause the output voltage to change. First, the ac line voltage is not constant. The so-called 115 V ac can vary from about 105 V ac to 125 V ac. This means that the peak ac voltage to which the rectifier responds can vary from about 148 V to 177 V. The ac line voltage alone can be responsible for nearly a 20 percent change in the dc output voltage. The second factor that can change the dc output voltage is a change in the load. In complex electronic equipment, the load can change as circuits are switched in and out. In a television receiver, the load on a particular power supply may depend on the brightness of the screen, the control settings, or even the channel selected. These variations in load tend to change the applied dc voltage because the power supply has a fixed internal impedance. If the load impedance decreases, the internal impedance of the power supply drops more voltage. This causes a decrease in the voltage across the load.

7.1 Conclusions

Switch-mode power supplies (SMPS's) not only convert energy, they also consume it. Typical operational efficiencies are about 25 to 60 % for linear power supplies and a bout 50-90% for switching power supplies. This means that products whose end-use electronics are dc like televisions and DVD players, could consume 50% less power during operating if the power supply were upgraded from 40% efficiency to 80% efficiency. Savings can occur not only from using SMPS's instead of linear power supplies, but also from specifying highly efficient switching power supplies. In many

cases, efficiencies are still lagging to keep costs down, since the power consumption is considered to be relatively low (40W-700W range). However, over time, efficiency improvement strategies will pay back based on the cost of energy. Therefore three common flyback converter topologies have been studied through this thesis in the Low (15W), Medium (40W), and High (150W) Power levels. Efficiency analyses on topologies showed the greatest opportunity for efficiency improvement to be in the 40W (medium power) topology and several approaches were investigated to determine the effects on the overall efficiency. It was determined that the medium-power stage of the topology could be modified for improved efficiency by pushing the output filter inductor parameters to the edge of their required ripple margin. Then, based on the new filter inductor values, the filter capacitor values were also recalculated, as well as the resulting output voltage ripple. This modification led to an efficiency improvement from 57.8% to 83.6%.

7.2 The Suggestion for Future Work

Additional research is needed to focus more attention on the input filter, feedback controller, transformer, and power switch, which also introduce losses, and thus the design of effective efficiency improvement. This thesis presents alternative options for efficiency improvement & measurement with the goal of improving the efficiency of switching power supplies. In addition, more efficiency enhancements are needed for low-power flyback converters.

BIBILIOGRAPHY

[1] M. Brown, *Power Supply Cookbook*. Newnes, 2001.

[2] A. von Jouanne, *An EPRI Report on Switch-Mode Power Supplies (SMPS's)*.2001

[3] J. T. Taylor Qiuting Huang, *CRC Handbook of Electrical Filters, CRC Press LLC*, 1997.

[4] A. I. Pressman, *Switching Power Supply Design*, McGraw-Hill, Inc, 1991.

[5] C. Calwell and T. Reeder, *A Hidden Opportunity for Energy Savings*, Ecos Consulting, 2002.

[6] S. S. Ang, *Power Switching Converters*, Dekker, 1995.

[7] M. J. Nave, *Power Line Filter Design For Switched-Mode Power Supplies*. Van Nostrand Reinhold, 1991.

[8] D. E. Johnson, *Introduction to Filter Theory*, Prentice-Hall, 1976.

[9] E. Christian, *LC Filters, Design, Testing, and Manufacturing*, Wiley Interscience,1983.

[10] M. G. ELLIS, SR, *Electronic Filter Analysis And Synthesis*, Artech House,1994.

[11] G. C. Chryssis, *High-Frequency Switching Power Supplies Theory And Design*, McGraw-Hill, 1989.

[12] L. E. Lawhite and M. F. Schlecht, "Active Filters for 1-MHZ Power Circuits with Strict Input/Output Ripple Requirements," *IEEE Transactins on Power Electronics*, 1987.

[13] R. P. Severns and G. Bloom, *Modern DC-TO-DC Switchmode Power Converter Circuits*, Rudolf P. Severns and Gordon Bloom, 1985.

[14] G. Chryssis, *High-Frequency Switching Power Supplies Theory and Design.* McGraw-Hill,1984.

[15] O. Kilgenstein, *Switched-Mode Power Supplies In Practice,* John Wiley and Sons, 1989.

[16] J. D. Lenk, *Simplified Design of Switching Power Supplies*, Butterworth-Heinemann, 1995.

[17] K. Billings, *Switch mode Power Supply Handbook*, McGraw-Hill, 1989.

[18] D. E. Johnson, *Introduction to Filter Theory*, Prentice-Hall, 1976.

[19] C. P. Basso, *Switch-Mode-Power Supply Spice Cookbook*, McGraw-Hill, 2001.

[20] K. Su, *Analog Filters Second Edition*, Kluwer Academic Pubilshers, 2002.

[21] L. J. Geis, *Transform Analysi And Filtersl*, Prentice-Hall, 1989.

[22] http://website.lineone.net/~colin_mccord/FYP/3.htm.

[23] "http://website.lineone.net/~colin_mccord/FYP/3.htm."

[24] "http://www.electronics-tutorials.com/filters/low-pass-filters.htm"

[25] N. Mohan, *T. M. Undeland and W. P. Robbins, Power Electronics Converters, Applications, and Design*, John Wiley and Sons, 1995.